Aircraft measurements of the impacts of pollution aerosols on clouds and precipitation over the Sierra Nevada

Daniel Rosenfeld,[1] William L. Woodley,[2] Duncan Axisa,[3] Eyal Freud,[1] James G. Hudson,[4] and Amir Givati[1]

Received 29 October 2007; revised 1 February 2008; accepted 4 March 2008; published 6 August 2008.

[1] Recent publications suggest that anthropogenic aerosols suppress orographic precipitation in California and elsewhere. A field campaign (SUPRECIP: Suppression of Precipitation) was conducted to investigate this hypothesized aerosol effect. The campaign consisted of in situ aircraft measurements of the polluting aerosols, the composition of the clouds ingesting them, and the way the precipitation-forming processes are affected. SUPRECIP was conducted during February and March of 2005 and February and March of 2006. The flights documented the aerosols and orographic clouds flowing into the central Sierra Nevada from the upwind densely populated industrialized/urbanized areas and contrasted them with the aerosols and clouds downwind of the sparsely populated areas in the northern Sierra Nevada. SUPRECIP found that the aerosols transported from the coastal regions are augmented greatly by local sources in the Central Valley resulting in high concentrations of aerosols in the eastern parts of the Central Valley and the Sierra foothills. This pattern is consistent with the detected patterns of suppressed orographic precipitation, occurring primarily in the southern and central Sierra Nevada, but not in the north. The precipitation suppression occurs mainly in the orographic clouds that are triggered from the boundary layer over the foothills and propagate over the mountains. The elevated orographic clouds that form at the crest are minimally affected. The clouds are affected mainly during the second half of the day and the subsequent evening, when solar heating mixes the boundary layer up to cloud bases. Local, yet unidentified nonurban sources are suspected to play a major role.

Citation: Rosenfeld, D., W. L. Woodley, D. Axisa, E. Freud, J. G. Hudson, and A. Givati (2008), Aircraft measurements of the impacts of pollution aerosols on clouds and precipitation over the Sierra Nevada, *J. Geophys. Res.*, *113*, D15203, doi:10.1029/2007JD009544.

1. Introduction

[2] Anthropogenic aerosols from major coastal urban areas pollute the pristine maritime air masses that flow inland from the sea and bring much of the precipitation, especially over the mountain ranges. Satellite observations indicated that urban aerosols reduce cloud drop effective radii (r_e) and suppress both warm and mixed phase precipitation in the clouds downwind of the urban areas [*Rosenfeld*, 2000]. This prompted studies that quantified the precipitation losses over topographical barriers downwind of major coastal urban areas in the western U.S (particularly in California) and in Israel. These results suggested losses of 15–25% of the annual precipitation over the western slopes of the hills [*Givati and Rosenfeld*, 2004, 2005; *Rosenfeld and Givati*, 2006; *Givati and Rosenfeld*, 2007; *Rosenfeld et al.*, 2007]. The suppression occurs mainly in the relatively shallow orographic clouds within the cold air mass of cyclones. The suppression that occurs over the upslope side is coupled with similar percentage enhancement on the much drier downslope side of the hills.

[3] These results are consistent with other studies that have shown that higher cloud condensation nuclei (CCN) concentrations increase cloud droplet concentrations, decrease cloud droplet sizes, reduce droplet coalescence and thus precipitation [e.g., *Hudson and Yum*, 2001; *McFarquhar and Heymsfield*, 2001; *Yum and Hudson*, 2002; *Hudson and Mishra*, 2007]. Therefore CCN from air pollution could be incorporated into orographic clouds, slowing down cloud-drop coalescence and riming on ice precipitation, hence delaying the conversion of cloud water into precipitation. The evidence includes significant decreasing trends of the ratio of hill/plains precipitation during the 20th century in polluted areas. Aerosol measurements from the IMPROVE aerosol monitoring network in the western U.S showed that the negative trends in the orographic precipitation are associated with elevated concentrations of fine aerosols (PM2.5). No trends are observed

[1]Institute of Earth Sciences, The Hebrew University of Jerusalem, Jerusalem, Israel.
[2]Woodley Weather Consultants, Littleton, Colorado, USA.
[3]Seeding Operation and Atmospheric Research, Plains, Texas, USA.
[4]Desert Research Institute, University of Nevada, Reno, Nevada, USA.

0148-0227/08/2007JD009544

in similar nearby pristine areas [*Givati and Rosenfeld*, 2004].

[4] In Central California the main precipitation suppression is postulated to occur during westerly flow that ingests anthropogenic CCN, which are incorporated into orographic clouds that form over the Sierra Nevada and are so shallow that their tops do not fully glaciate before crossing the mountain crest. This means that at least some of the water in these clouds remains in the form of cloud droplets that are not converted to precipitation (or at least ice hydrometeors) before crossing the divide, and hence re-evaporate after producing some precipitation on the downwind side of the crest. Recent model simulations support this hypothesis [*Lynn et al.*, 2007; *Woodley Weather Consultants*, 2007].

2. SUPRECIP Program

[5] Following the publication of many of the recent findings cited above a research effort called the Suppression of Precipitation (SUPRECIP) Program was conducted to make in situ aircraft measurements of the polluting aerosols, the composition of the clouds ingesting them, and the way the precipitation-forming processes are affected. The SUPRECIP field campaigns were aimed at making the measurements necessary for the validation of the above hypothesis that urban air pollution suppresses orographic precipitation.

[6] SUPRECIP was conducted during February and March of 2005 (SUPRECIP 1) and February and March of 2006 (SUPRECIP 2). The Seeding Operations and Atmospheric Research (SOAR) Cheyenne II, turbo-prop, cloud physics research aircraft was used in SUPRECIP-1; the Cheyenne and an additional (SOAR) Cessna 340 aerosol aircraft were flown in SUPRECIP-2. These aircraft were used to measure atmospheric aerosols in pristine and polluted clouds and the impact of the aerosols on cloud base microphysics, on the evolution with height of the cloud drop-size distribution and on the development of precipitation under warm and mixed-phase processes. They were used also to validate the multispectral satellite inferences of cloud structure and the effect of pollutants on cloud processes, especially the suppression of precipitation. This research effort is funded by the PIER (Public Interest Energy Research) Program of the California Energy Commission.

[7] The Cheyenne II cloud physics aircraft that was used in SUPRECIP is shown in Figure 1. The instruments and respective data sets taken by the aerosol and cloud physics airplanes are given in Tables 1 and 2, respectively. The flights of these aircraft documented the aerosols and orographic clouds downwind of the densely populated areas in the north-central Sierra Nevada and contrasted them with the aerosols and clouds downwind of the sparsely populated areas in the far northern Sierra Nevada.

2.1. SUPRECIP-1 Effort

[8] The focus of SUPRECIP was on the nature and source of the pollution aerosols that ancillary analyses had suggested to be decreasing the orographic component of precipitation in the California Sierra Nevada. These aerosols are tiny cloud condensation nuclei (CCN). High CCN concentrations reduce droplet sizes and thus inhibit precipitation-forming coalescence processes and ultimately the riming of ice crystals [*Borys et al.*, 2000, 2003]. According to the satellite inferences the decreases in r_e are taking place over the central and southern Sierra where the losses in precipitation and stream flows have been documented [*Woodley Weather Consultants*, 2005] but not in the far northern Sierra where no such changes were noted. The next step in the overall investigation was to determine whether the satellite-inferred cloud properties, especially the r_e, could be validated by actual measurements by a cloud physics aircraft within the subject clouds. This was a primary motivation for SUPRECIP-1.

[9] The weather during SUPRECIP 1 was highly anomalous for the entire U.S. West Coast with dry conditions in the Pacific Northwest and flooding rains in Southern California. A high-pressure blocking pattern at the surface and aloft-tended to split the jet streamflow to the north or south of the northern Sierra. This persistent region of low pressure under the block produced southerly and southeasterly winds and long periods of middle and high clouds over the Central and Northern Sierra for most of the project. The desired orographic clouds produced by the usual westerly winds into the Sierra were a rarity during SUPRECIP 1. Therefore the program was extended through the first week in March.

[10] The use of the Cheyenne II, turbo-prop, cloud-physics aircraft provided documentation of differences in cloud microphysics associated with differences in CCN that were visibly related to air pollution. It was also determined that these differences were consistent with satellite retrievals. This is crucial since, previously, only the satellite retrievals were available as indicators of the apparent negative effect of pollution on Sierra precipitation, as published initially for Australia [*Rosenfeld*, 2000] and later for the Sierra [*Woodley Weather Consultants*, 2007]. Thus the new aircraft measurements could be used to validate the satellite inferences of cloud microphysics by showing the negative impact of pollutants on cloud processes and precipitation. The aircraft and satellite measurements in SUPRECIP showed that some of the Sierra precipitation was produced by surprisingly shallow pristine clouds. This suggested that pollution may help explain the long-term losses in Sierra orographic precipitation.

[11] To provide better comparisons with aircraft data satellite inferences of r_e were made for cloud pixels in a series of boxes along the aircraft flight tracks. These provided comparisons of median r_e for the cloud passes at the height and temperature of each pass. The results are given in Figure 2, which shows a scatterplot of r_e measured by the cloud physics aircraft versus the inferences of r_e from the satellite imagery (Satellite median r_e) for 2 d of study in SUPRECIP-1. Considering the differences in scale (i.e., individual cloud passes versus the composite clouds within a box that contains the cloud passes) and time, the agreement is reasonable (linear correlation = 0.73). The regions of California that experienced losses in precipitation and streamflow had decreased r_e values compared to r_e for more pristine areas of California. Although it seemed reasonable to ascribe the decreased droplet sizes to the ingestion of pollution aerosols, such causality had not been proved.

[12] Additional analyses were made for those days with complete cloud microphysical data sets, including time, altitude and temperature of the cloud passes, the CDP

Figure 1. The SOAR Cheyenne II cloud physics aircraft.

(cloud droplet probe) LWC, mean and maximum droplet concentrations, and median r_e for each cloud pass. The CIP (cloud imaging probe) instrument provided an estimate of the precipitation water. Aerosol information was supplied by the CCN counter operated at 0.5% supersaturation (S). The total aerosols as a function of size were provided by Texas A&M University's aircraft-based high flow rate Differential Mobility Analyzer (DMA)/Tandem Differential Mobility Analyzer (TDMA).

[13] The SUPRECIP-1 data were used to show an association between the CCN concentrations and the in-cloud droplet concentrations before and after each cloud pass at the same altitude. Figure 3 shows a scatterplot and regression analysis of in situ droplet concentrations (mean and maximum) and CCN concentrations - before and after the cloud penetrations at the same altitude. This figure shows that the greater the CCN concentration around the cloud - the greater the in-cloud droplet concentrations. Thus aerosols would appear to have a direct effect on in-cloud microphysics.

[14] The next step was to relate the CCN concentrations to the effective diameter (Deff) of the cloud droplets. This

Table 1. Data Sets From the Aerosol Aircraft

Variable	Instrument	Range	Accuracy	Resolution	Frequency
Air temperature	Rosemount 102DB1CB	−50°C to +50°C	0.1°C	0.01°C	1 Hz
Liquid water content	DMT LWC-100	0 to 3 g/m^3	0.05 g/m^3	0.01 g/m^3	1 Hz
Logging, telemetry & event markers	ESD DTS (GPS)				1 Hz
Isokinetic aerosol inlet	Brechtel double diffuser inlet	28 lpm			100 m/s
CN concentration	TSI 3022A	>2 nm		0–10^5/cm^3	1 Hz
CCN	DMT CCN counter	0.5 to 10 μm			
		0.1 to 1.2 % SS	0.5 μm, 20 bins	1 Hz	

Table 2. Data Sets From the Cloud Physics Aircraft

Variable	Instrument	Range	Accuracy	Resolution	Frequency
Air temperature	Rosemount 102DB1CB	−50°C to +50°C	0.1°C	0.01°C	1 Hz
Air temperature(Reverse flow)	0.038″DIA. dead thermistor	−30°C to +50°C	0.05°C/0.3°C incl DHC	0.01°C	<1 s TC
Relative humidity (reverse flow)	thermoset polymer RH sensor	0 to 100% RH	2% RH	0.1% RH	5 s TC @ 20°C
Barometric pressure	MEMS pressure sensor	0 to 110000 Pa	100 Pa	10 Pa	20 Hz
u wind component (+ North)	Extended Kalman Filter (EKF)		0.50 m/s @ 75 m/s TAS	0.01 m/s	5 Hz
v wind component (+ East)	Extended Kalman Filter (EKF)		0.50 m/s @ 75 m/s TAS	0.01 m/s	5 Hz
w wind component (+ Down)	Extended Kalman Filter (EKF)		0.50 m/s @ 75 m/s TAS	0.01 m/s	5 Hz
Position (latitude/longitude)	WAAS DGPS		2 m (2σ)	<1 m	5 Hz
Altitude	WAAS DGPS	−300 to 18000 m	5 m (2σ)	<1 m	5 Hz
Geometric altitude	King KRA 405 radar altimeter	0 to 2000 ft	3% < 500 ft 5% > 500 ft	0.48 ft (0.15 m)	
Roll attitude (ϕ)	MEMS IMU/GPS/EKF	−60 to +60°	0.1°	0.01°	5 Hz
Pitch attitude (θ)	MEMS IMU/GPS/EKF	−60 to +60°	0.2°	0.01°	5 Hz
Yaw attitude (ψ)/heading	MEMS IMU/GPS/EKF	0 to 360°	0.1°	0.01°	5 Hz
Angle of attack (α)	MEMS pressure sensor	−15 to +15°	0.03° @ 150 m/s	0.001° @ 150 m/s	20 Hz
Side-slip (β)	MEMS pressure sensor	−15 to +15°	0.03° @ 150 m/s	0.001° @ 150 m/s	20 Hz
True air speed	MEMS pressure sensor	0 to 150 m/s	0.1 m/s	0.01 m/s	20 Hz
Logging, telemetry & event markers	ESD DTS (GPS)				1 Hz
Cloud droplet spectra	DMT CDP	2 to 50 μm		1 to 2 μm, 30 bins	1 Hz
	PMS FSSP SPP-100	2 to 47 μm		1 to 2 μm, 30 bins	1 Hz
Cloud particle spectra	DMT CIP 1D	25 to 1550 μm		25 μm, 62 bins	1 Hz
Cloud particle image	DMT CIP 2D	25 to 1550 μm		25 μm	
Liquid water content	DMT LWC-100	0 to 3 g/m^3	0.05 g/m^3	0.01 g/m^3	1 Hz
	CDP calculated	>3 g/m^3			1 Hz
	FSSP calculated	>3 g/m^3			1 Hz
CN concentration	TSI 3010	>7 nm		0–10^5/cm^3	1 Hz

requires normalization to the cloud LWC with the expression Deff/LWC$^{0.333}$ for each cloud pass. This normalization is needed because Deff and LWC generally increase with distance above cloud base. Variations in cloud-penetration distances above cloud base need to be accounted for in order to make valid comparisons with CCN. The ratio with LWC is used because cloud base height and/or distance from cloud base are seldom known. LWC$^{0.333}$ is used

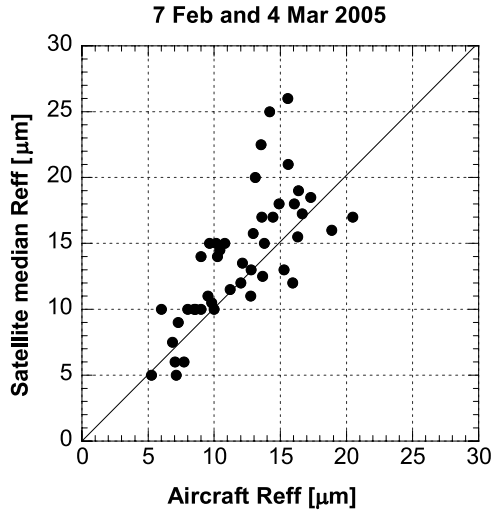

Figure 2. Scatterplot of the median effective radii (r_e) determined by aircraft (Aircraft Reff) for individual cloud passes versus the median r_e inferred from the multispectral satellite imagery (Satellite median Reff) for the altitudes and temperatures of the aircraft cloud passes for clouds within boxes that contain the cloud passes. The comparisons were made for data obtained on 7 February and 4 March 2005.

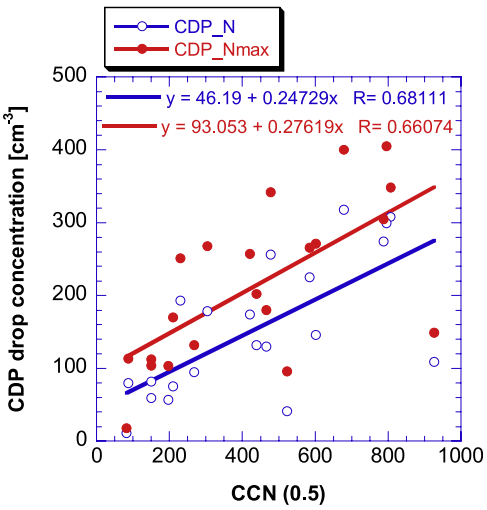

Figure 3. Cloud drop number concentrations as a function of the CCN concentration at a supersaturation of 0.5%. Each point represents the median (blue) and maximum (red) droplet concentrations for one cloud pass. The best fit equations are as shown. The data are from the afternoon flight of 28 February 2006.

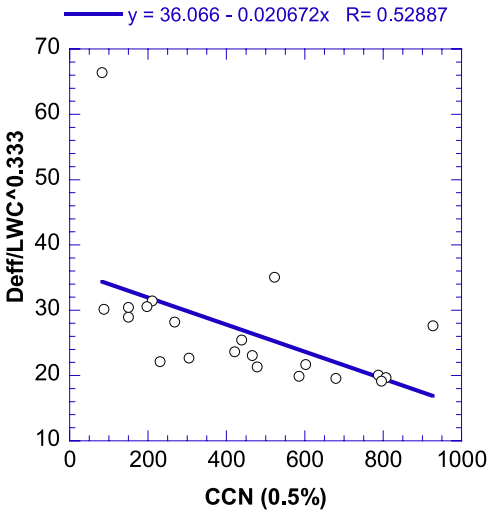

Figure 4. The effective diameter (Deff) of the cloud drops normalized to the cloud liquid water (LWC) content by the expression $Deff/LWC^{0.333}$, as a function of the CCN concentrations for each cloud pass. The data are from the afternoon flight of 28 February 2006.

because this is generally proportional to Deff (droplet diameter relates to the cube root of the volume). The CCN concentrations were taken from the immediate clear air vicinity of the cloud passes. The negative relationship is given by the regression equation. Figure 4 shows that Deff decreases as the CCN concentration increases. Thus air pollution CCN decrease cloud droplet sizes.

[15] In summary, the flights of SUPRECIP-1 documented the aerosols and orographic clouds in the central Sierra Nevada and contrasted them with the aerosols and clouds downwind of the sparsely populated areas in the northern Sierra Nevada. The main results from SUPRECIP-1 are [*Woodley Weather Consultants*, 2005].

[16] ● The in situ aircraft measurements of the cloud microphysics validated the satellite retrievals of r_e and microphysical phase.

[17] ● Ample supercooled drizzle drops were found in the pristine orographic clouds with only few tens of drops cm^{-3}, and no drizzle with small concentrations of graupel were found in clouds with drop number concentrations of $\sim$150 cm^{-3}.

[18] ● The pristine clouds occurred in air masses that were apparently decoupled from the boundary layer in the early morning, whereas the more microphysically continental clouds occurred during the afternoon after the surface inversion over the Central Valley disappeared.

[19] Despite the accomplishments of SUPRECIP-1, all of its objectives had not been met because of incomplete documentation of the aerosols in the atmospheric boundary layer, due to the near impossibility of obtaining clearance to conduct flight under instrument flight rules (IFR) in the boundary layer in the San Francisco/Oakland/Sacramento heavily populated urban and industrial areas. A second aircraft flying under visual flight rules (VFR) would have been necessary to obtain the needed documentation. In addition, the lack of orographic cloud conditions over the California Sierra due to weak wind flow into the Sierra during virtually all of the period of flight operations was a major problem. A longer period of operations would have been required to obtain the desired orographic clouds.

2.2. SUPRECIP-2 Effort

[20] A second field campaign (SUPRECIP 2) was conducted in February and March 2006 to better document the aerosol effect on clouds. The cloud physics instrumentation was enhanced with another cloud droplet spectrometer (FSSP SPP-100), and a second low-level aerosol airplane was added. Two research aircraft were involved, making measurements of CCN, CN, cloud drop size distribution, hydrometeor images and size distributions, the thermodynamic properties of the air and air 3-D winds. Information about the CN and CCN instrumentation on the aerosol aircraft and the CN instrument on the cloud physics aircraft is provided in Tables 1 and 2, respectively. SUPRECIP-2 was augmented also by surface measurements of aerosols and chemical composition of the hydrometeors, made by collaborating research groups from the Desert Research Institute of the University of Nevada, The University of California Davis, and the SCRIPPS Oceanographic Institute of the University of California at San Diego. This provided coincident measurements of the low level aerosols and the properties of the clouds that ingest them. The results reported here confirm the link between anthropogenic aerosols and the suppression of precipitation-forming processes in California clouds.

[21] The aerosol aircraft operated below the bases of the clouds that the cloud physics aircraft monitored. This provided measurements of the aerosol that was ingested into these clouds. The SUPRECIP 2 project goal was measurement of atmospheric aerosols in pristine and polluted clouds and documentation of the impact of the aerosols on cloud base microphysics, on the evolution with height of the cloud drop-size distribution and on the development of precipitation under warm and mixed-phase processes. The objectives in the context of this goal included:

[22] ● Systematically "mapping" the pollution aerosols at low to mid levels in urban and downwind areas using both research aircraft.

[23] ● Documenting the connection between the aerosols and the measured cloud microphysics and precipitation forming processes.

[24] ● Validating the multispectral satellite inferences of cloud structure and the effect of pollutants on cloud processes, especially the suppression of precipitation.

[25] During SUPRECIP-2 53 research missions were flown, 25 by the cloud physics aircraft and 28 by the Cessna 340 aerosol aircraft. A little over half (27 of 53) of the research missions were flown in March 2006, when the weather was much more favorable (10 flight days) than February.

3. Results of SUPRECIP 2 Analyses

3.1. Establishing a Direct Link Between the Subcloud Aerosols and Cloud Microphysical Structure

3.1.1. A Case Study

[26] The linkage between ingested subcloud aerosols and cloud microphysics is best illustrated by a case study on the afternoon of 28 February 2006. A cold front had passed

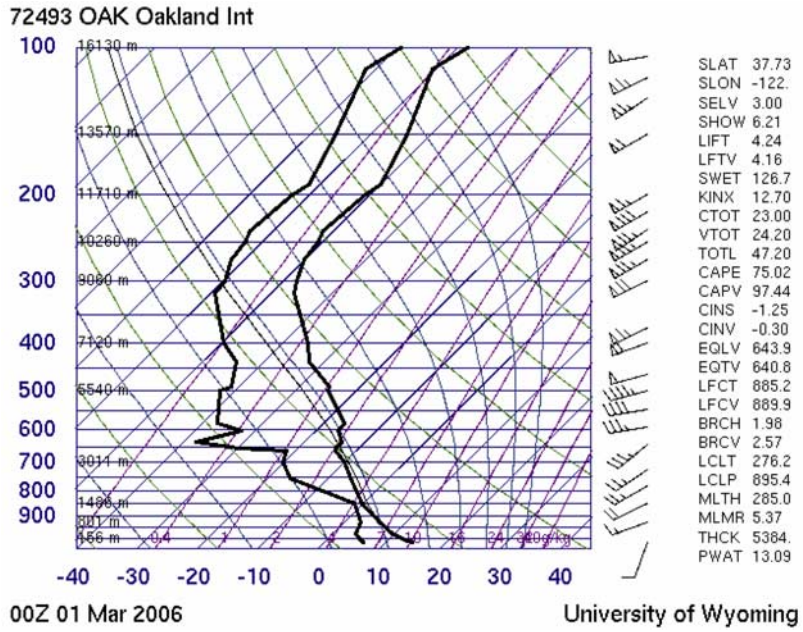

Figure 5. The Oakland radiosonde of 1 March 2006 at 00Z, which is near the time that the aircraft flew near Oakland.

through the area the previous night and a postfrontal cold air mass moved from the west southwest over all of Central California by the following afternoon. Postfrontal instability caused convective clouds over the ocean, and triggered convective clouds over the coastal hills and over the Sierra Nevada. Although the instability decreased gradually during the day, rain showers from shallow clouds were still occurring over the ocean and the coastal ranges at 00Z on 1 March 2006. Figure 5 shows the Oakland radiosonde at that time.

[27] A coordinated mission of the Cloud and Aerosol airplanes originated from the Sacramento Executive Airport to document the gradient in aerosols and cloud properties by doing cross sections from the Sierra Nevada to and from the Pacific Ocean. The aircraft departed Sacramento at 23:05Z and flew due east to the foothills and measured the convection generated there by the mountains. The next destination was the clouds that formed over the hills bounding the Central Valley to its west, about 60 km to the NE of Monterey. Next the aircraft sampled the clouds forming over the hills just at the Pacific coast at Big Sur. There the aircraft continued 35 km westward over the ocean and then turned north to measure convective clouds that were triggered by the ocean shoreline of San Francisco. Then the aircraft turned east over the north part of San Francisco Bay and measured a cloud just inland over Richmond, and then another cloud over Sacramento before finally landing. The tracks of the two aircraft and the locations of the measured clouds are provided in Figure 6.

[28] The aerosol aircraft measurements are summarized in Figure 6. Because the supersaturation (or the temperature difference between the plates, dT) in the Cloud Condensation Nuclei Counter cycles every ~7 min, there was a need to correct the CCN data measured at low supersaturations to a common SS. Without correction or adjustment there would be too few data points measured at the same SS. In order to do this, it was necessary to find the relation between dT (instead of SS) and the CCN concentration for each flight separately, because this relation might be affected by the chemical composition of the aerosols, their sizes and their concentrations. After determining and applying the correction, the CCN concentrations were plotted for an entire flight to a common 0.85% SS for measurements in the boundary layer. On average, the ratio of CCN counts at super saturations of 0.85% and 0.5% was 1.89 with a standard deviation of 0.4.

[29] The aircraft aerosol measurements show CCN concentrations varying between 300 and 800 cm^{-3} over the first section to the SE at the western slopes of the Sierra Nevada. The CCN concentrations fell to about 100 cm^{-3} over the hills 60 km NE of Monterey, and continued falling to less than 40 cm^{-3} over Monterey Bay and likely also over Big Sur. The CCN increased again gradually to the north along the coastline and reached about 70 cm^{-3} there. They kept rising to about 100 cm^{-3} over the peninsula of San Francisco airport, and jumped locally to 800 cm^{-3} just to the north of the airport, but recovered back to less than 80 cm^{-3} to the north of the Golden Gate Bridge. The aircraft turned to the east and experienced a sharp increase of the CCN to more than 700 cm^{-3} over Richmond. The condensation nuclei (CN) then shot up > 10,000 cm^{-3}. This suggests an ample source of fresh small aerosols. The CCN remained generally above 500 cm^{-3} within the boundary layer all the way to landing in Sacramento.

[30] The cloud- and precipitation particle size distributions are given in Figures 7–11. Cloud 1 was sampled stepping upward from base through its upshear towers, whereas its more mature portions glaciated and precipitated. Because of air traffic control limitations it was necessary to use different clouds in the same area for the lower and upper portions of the cross sections. The modal liquid water cloud drop diameter (DL, defined as the drop diameter having the greatest LWC) increased with height above cloud base. It

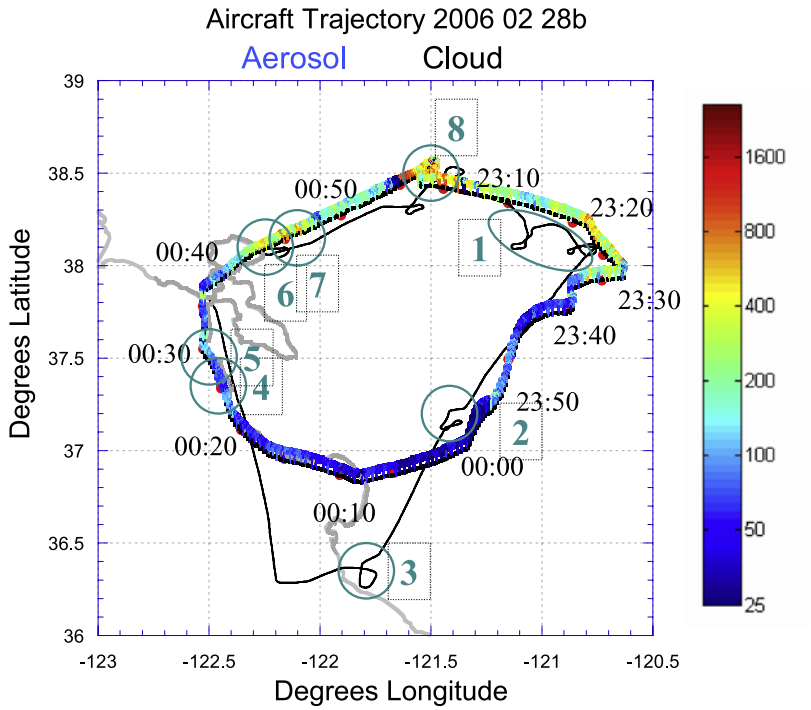

Figure 6. The tracks of the Cloud (black) and Aerosol (colored) airplanes. The time marks every 5 min are posted on the aerosol aircraft trajectories, and labeled every 10 min. The CCN concentrations adjusted to supersaturation of 0.9% are shown in the color scale. The relative height of the aerosol aircraft above sea level is shown by the vertical displacement of the track. The measured clouds by the cloud physics aircraft are marked with green circles and numbered sequentially.

reached 21 μm at the altitude of 3635 m, which is about 1900 m above cloud base. The temperature there was -8°C. This size is below the DL threshold for the development of warm rain that was documented elsewhere as 24 μm [*Andreae et al.*, 2004]. In agreement with that, the DL did not expand to drizzle size. Large precipitation particles occurred as graupel and formed a well separated distribution at the 1-mm size range.

[31] From the location of Cloud 1 the aircraft was flown diagonally to the southwest and across the Central Valley. The valley was mostly cloud-free, except for some midlevel layer clouds. The next area of clouds was triggered by the ridge that bounds the Central Valley on its west. The cloud tops had a convective appearance and were sampled at the lowest allowed altitude - (2100 m, to provide safe- ground clearance over the highest terrain) up to the cloud tops at 2700 m. The temperature there was -3°C, but the maturing clouds were visibly turning into a diffused fibrillation texture, indicating the conversion of the cloud water to precipitation and/or ice crystals. Glaciation would be in such case produced probably by a mechanism of ice multiplication. The modal LWC drop size was 28 μm at 2100 m and reached 33 μm at the cloud top at 2700 m. This is clearly beyond the threshold (DL = 24 μm) for warm rain [*Gerber*, 1996; *Yum and Hudson*, 2002]. In agreement with that, the cloud droplet size distribution (DSD) was extended smoothly to the drizzle and small raindrop sizes, as measured by the CIP and presented in the lower panel of Figure 9. The appearance of the warm rain is consistent with the decrease of the CCN concentrations to about 100 cm^{-3}.

[32] The aircraft continued flying to the SW to the next area of clouds (cloud 3). These were triggered by the coastal hills near Big Sur. The aircraft stepped vertically through the convective- looking cloud tops from the lowest safe height of 1880 m to their tops at a height of 2250 m at temperature of -3°C. The CCN concentrations as measured by the aerosol aircraft in Monterey Bay varied between 20 and 50 cm^{-3}. These low CCN concentrations produced large cloud drops ranging from a modal LWC drop diameter of 30 μm at 1880 m to 43 μm at the cloud tops. The DSD extended smoothly into drizzle and small raindrops (see Figure 8). Large hydrometeors were nearly absent. The cloud drops were so large so that the solar radiation reflected from the particles near the cloud top formed a cloud bow. These clouds had clearly created active warm rain.

[33] From Big Sur the flight continued over the ocean and then turned north and flew at a constant altitude across Monterey Bay to the Golden Gate and then eastward back to Sacramento. This flight path took the aircraft along an aerosol gradient that increased from pristine over the ocean to polluted air just to the east of San Francisco Bay. Convective clouds grew along that flight path and reflected the impact of the changing CCN concentrations at that fixed altitude. Clouds 4 to 8 were penetrated along this gradient flight (Figure 9).

[34] Cloud 4 was penetrated at the coastline of the peninsula to the west of San Francisco. The CCN concentration there was about 70 cm^{-3} and the cloud had a DL of 31 μm and created warm rain. A faint cloud bow was barely visible. Cloud 5 was penetrated a short distance to the north,

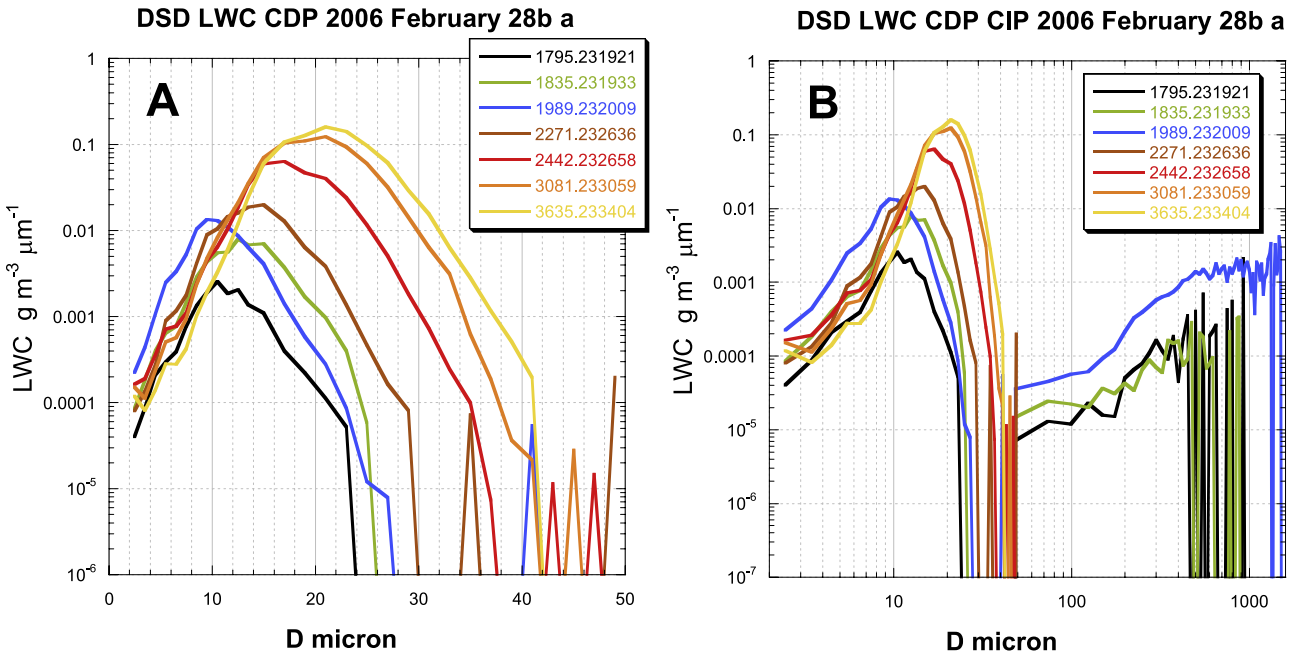

Figure 7. Plot of cloud droplet diameters as a function of liquid water content (LWC) for Cloud 1 over the western slopes of the Sierra Nevada (see location in Figure 6). The modal liquid water drop diameter occurs at the droplet size having the greatest water content. Cloud 1 developed in an air mass that had 300–800 CCN cm^{-3}. Panel A shows the Cloud Droplet Probe (CDP) measured LWC distribution. Each line represents the gross cloud drop size distribution of a whole cloud pass. The legend of the lines is composed of the pass height [m] to the left of the decimal point, and the pass starting GMT time [hhmmss] to the right of the point. The passes are ordered in altitude ascending order. Note the increase in cloud drop volume modal size with increasing cloud depth. Panel B shows the combined distributions of the CDP and the cloud imaging probe (CIP). According to the figure the large precipitation particles were well separated from the cloud drop size distribution, indicating lack of appreciable coalescence.

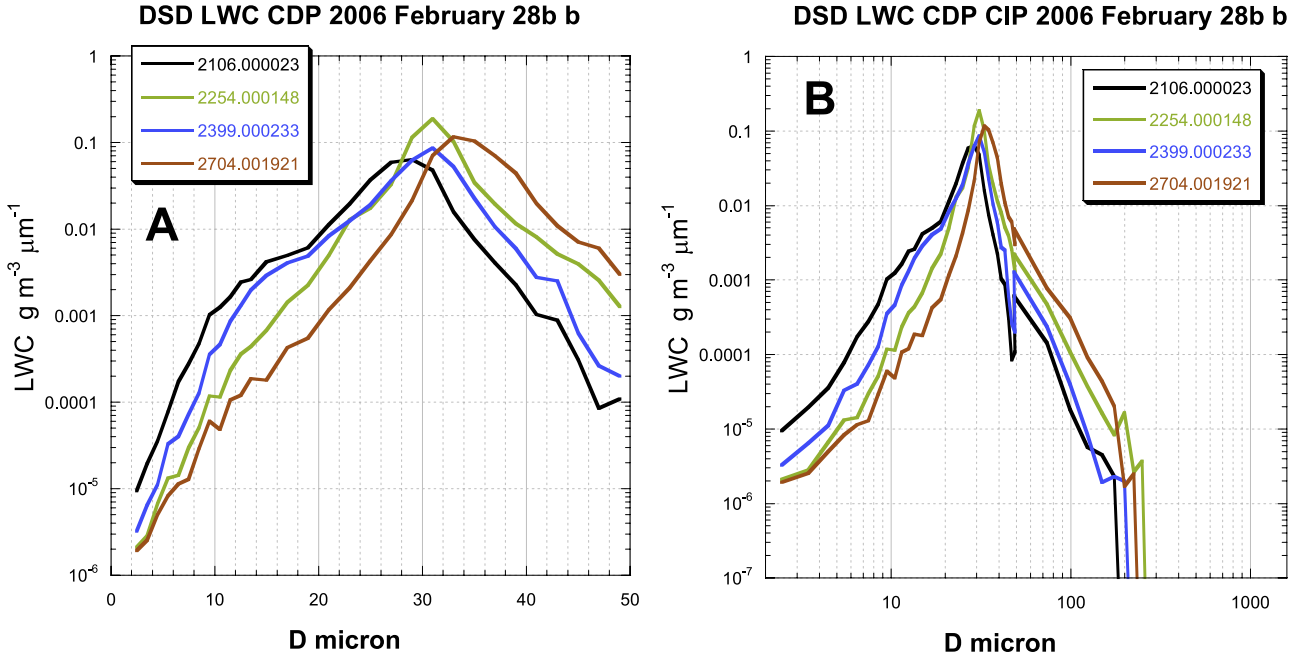

Figure 8. Same as Figure 7, but for Cloud 2 over the hills 60 km NE of Monterey (see location in Figure 6). It developed in an air mass that had 100 CCN cm^{-3}. The cloud drops are quite large and the distribution continues smoothly into the raindrop sizes. This indicates active warm rain processes.

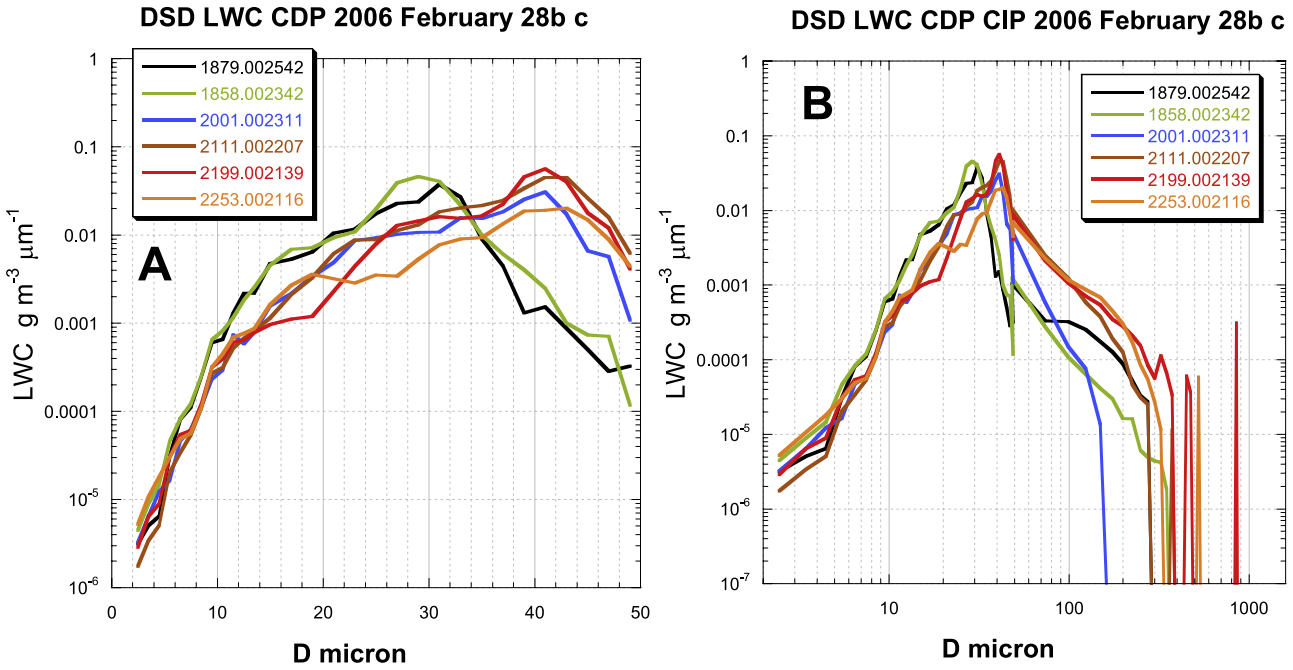

Figure 9. Same as Figure 7, but for Cloud 3 over the hills near Big Sur (see location in Figure 6). It developed in an air mass that had about 40 CCN cm^{-3}. The cloud drops are very large and the distribution continues smoothly into the raindrop sizes. This indicates very active warm rain processes.

where the CCN increased to 100 cm^{-3}. Cloud 5 still had warm rain, but to a lesser extent than Cloud 4. Shortly after passing directly over San Francisco International airport, over the Golden Gate Bridge, a short jump in the CCN occurred to about 600 cm^{-3} and recovered to the background of <70 cm^{-3}.

[35] The aircraft turned east and crossed the northern arm of San Francisco Bay. The CCN concentrations increased to

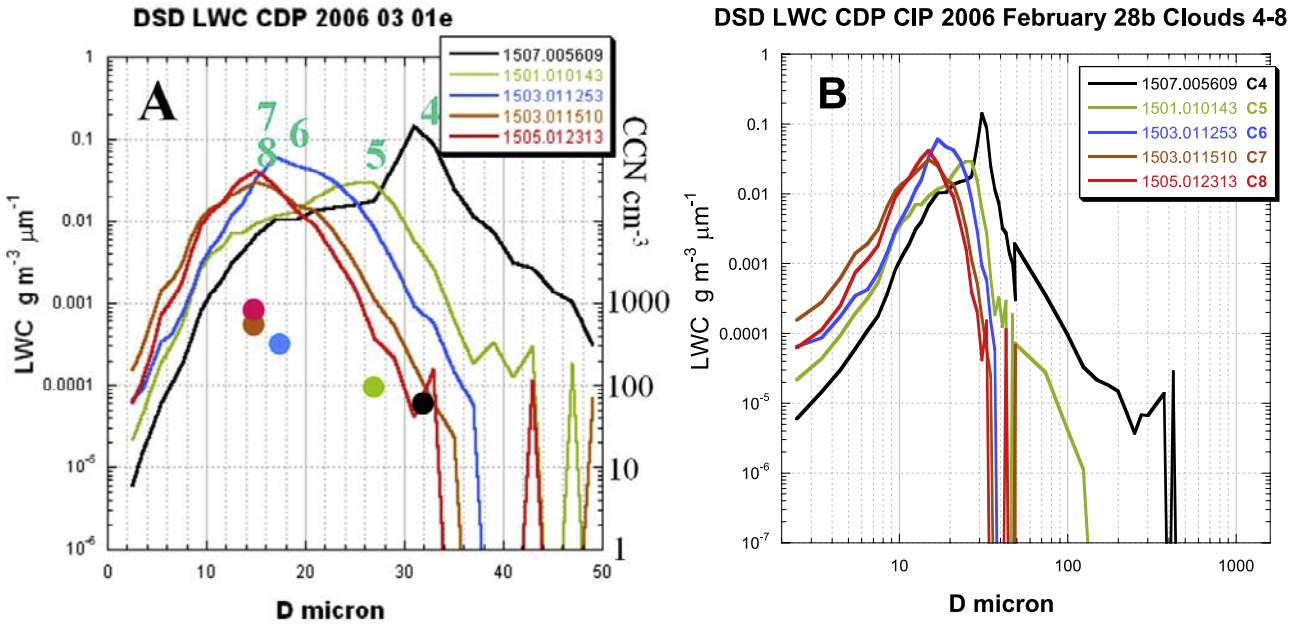

Figure 10. Same as Figure 7, but for single heights in clouds 4–8 in a cross-section from the Pacific Ocean to Sacramento, marked by C4, C5, C6, C7, and C8 respectively. The respective approximated CCN concentrations from the measurements made by the aerosol aircraft are denoted by the circles and are located under the peaks of the DL plots having the same color. The CCN values are to be read from the right ordinate. The CCN concentrations are: C4: 70, C5: 100, C6: 300, C7: 600, C8: 800 cm^{-3}. The drops become markedly smaller with increasing CCN concentrations. Warm rain ceases at cloud 3 where 300 CCN cm^{-3} were present.

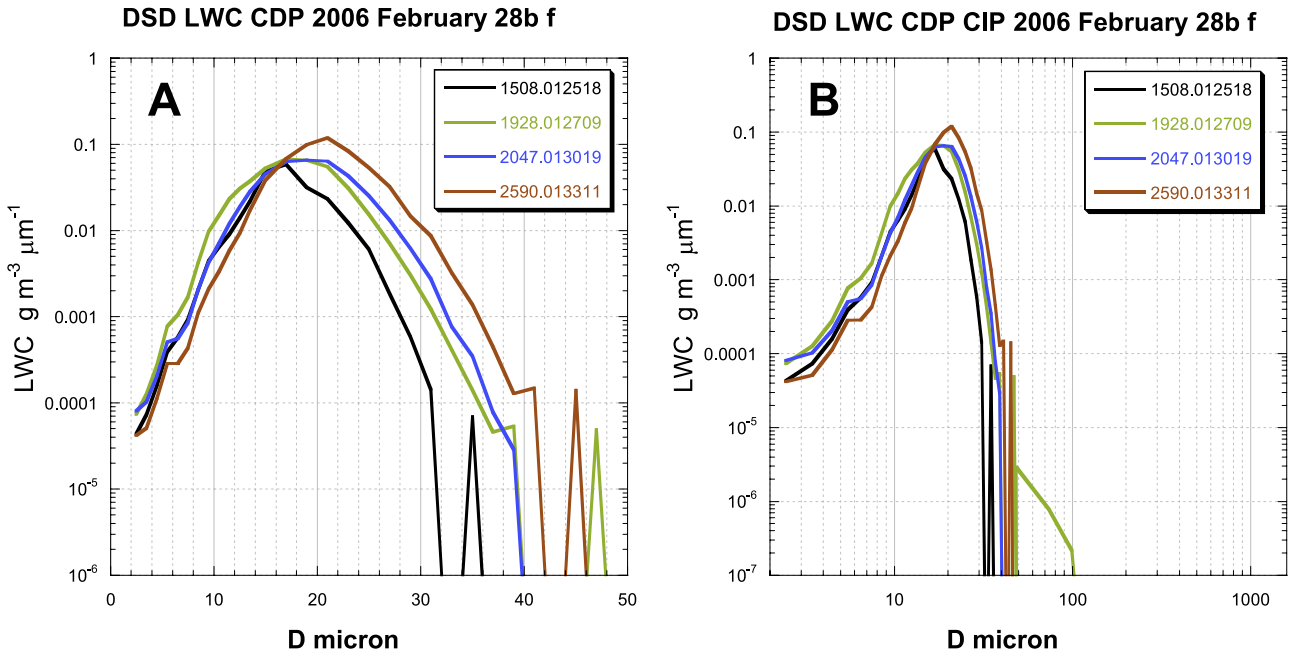

Figure 11. Same as Figure 7, but for the vertical cross section in Cloud 8 over Sacramento (see location in Figure 6). It developed in an air mass that had about 800 CCN cm^{-3}. The cloud drops are very small and do not expand much with height into raindrops, again as in Cloud 1.

about 300 cm^{-3} shortly after crossing the coast line. Cloud 6 formed over the eastern part of Richmond. Its modal LWC DSD decreased to 17 μm, well below the warm rain threshold of 24 μm. The CIP confirmed that this cloud had no precipitation particles. This occurred less than an hour after the time of the Oakland sounding at 00Z, which represented pretty well the local conditions and showed light southwesterly winds near the surface that veered to stronger west-southwest winds at the higher levels.

[36] Cloud 7 occurred a few km farther east of cloud 6, where the CCN concentrations increased to 600 cm^{-3}. Its DL decreased further to 15 μm. Cloud 8 developed farther east over Sacramento, where the CCN concentration varied between 600 and 1000 cm^{-3}. The cloud had a similar microphysics to cloud 7. A vertical stepping through cloud 8 showed little widening of the DSD with height (Figure 11), which serves as an additional indication of the scarcity of coalescence in that cloud.

[37] A satellite analysis (Figure 12) shows that the satellite retrieved microphysics of the cloud field is in agreement with the in situ measurements that suggest suppression of precipitation in Area 1, which includes Cloud 1, while showing ample warm rain in Area 8, which includes Cloud 3.

[38] In summary, a detailed analysis of a single flight of SUPRECIP 2 showed a clear relationship between CCN concentrations, cloud microphysics and precipitation forming processes. The distribution of the CCN showed an unambiguous urban source, at least in the San Francisco Bay area. The role of the anthropogenic aerosols is demonstrated by the contrast between Cloud 2 some 50 km inland in a relatively sparsely populated area, compared with clouds 6 and 7 only several km inland over the heavily populated and industrialized Bay area. While Cloud 2 was quite pristine and produced ample coalescence and warm rain, coalescence in cloud 7 was highly suppressed and it produced no precipitation.

[39] The differences in the anthropogenic CCN likely explain the observed differences. Cloud base temperature over the coast (San Francisco) was warmer by about 2°C than the cloud base inland (Sacramento). This cannot explain the observed differences in the clouds microstructure for the same height above cloud base, because it incurs a difference of less than 10% in the amount of adiabatic water for the same height above cloud base for the heights of interest. The fastest growth of DL in near the coast line cannot be explained by the probable greater abundance of sea-spray generated giant CCN, because they would act to enlarge the tail of the cloud DSD and not its mode. Furthermore, both cloud base temperature and sea salt CCN should change at the same rate with distance from the coast over the urban and rural areas. Differences in land use would, if anything, contribute to the opposite effects with respect to the actually observed. The mountains at the coast line near Big Sur should enhance the updraft and cause smaller cloud drops and less coalescence, but in fact the largest drops and strongest warm rain were observed there. The urbanized area should have provided more sensible heat for greater updrafts, but this should play a minimal role with the weak winter solar heating. Therefore there is no probable mechanisms that can explain the observed differences in the cloud microstructure and precipitation properties to which the authors are aware of, except for the differences in the anthropogenic CCN.

[40] The satellite image (Figure 12), taken 3 to 4 h before the flight, supports the aircraft observations and shows that an even greater source than the urban San Francisco Bay area for aerosols occurred in the central and southern Central Valley. A flight earlier in the day measured CN concentrations exceeding 20,000 cm^{-3} and CCN concen-

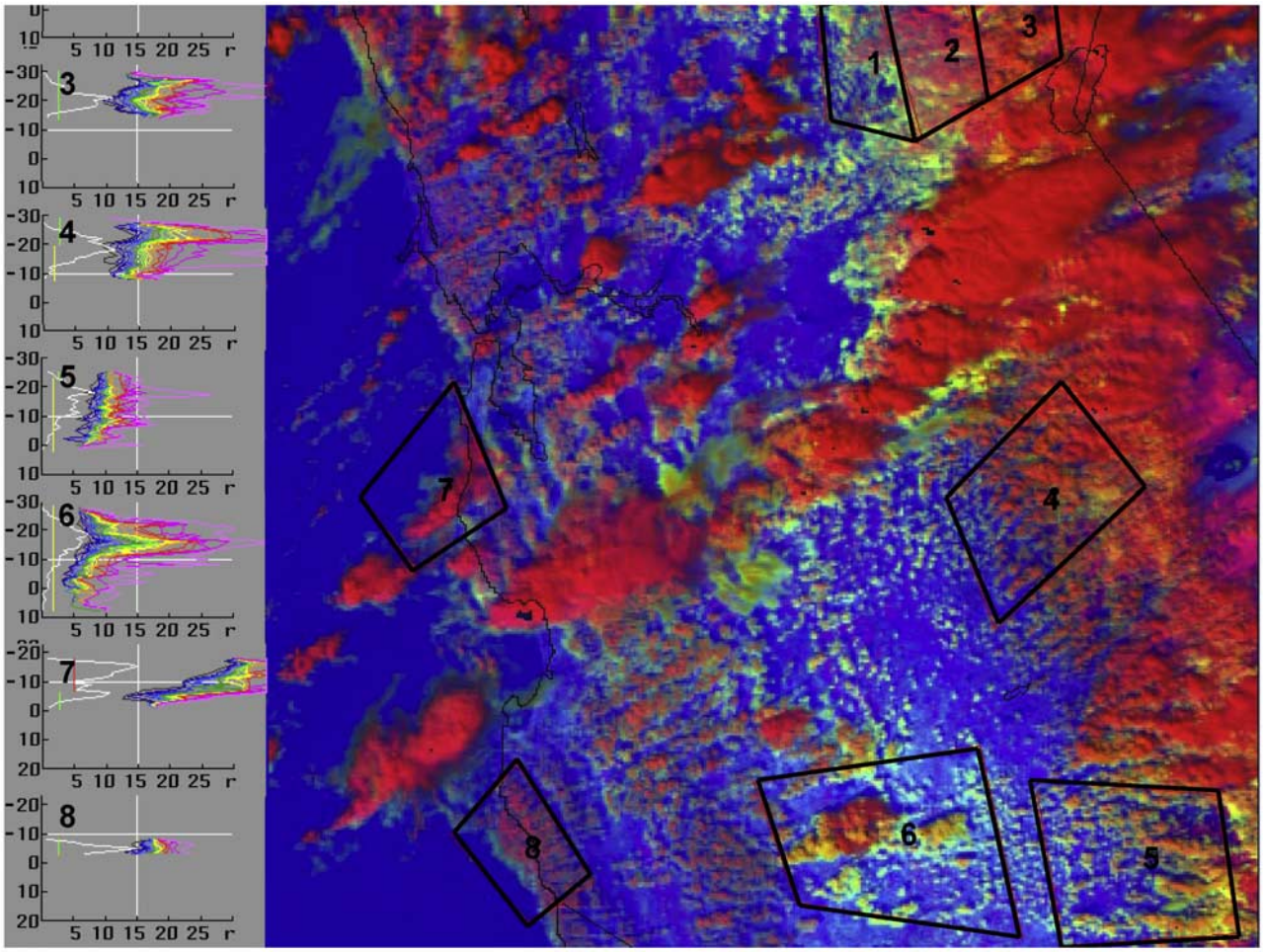

Figure 12. Aqua MODIS image of the clouds in central California on 2006 02 28 at 21:00Z. The color scale is a composite following *Rosenfeld and Lensky* [1998] where the red is modulated by the visible solar reflectance, blue modulated by the thermal temperature, and green modulated by the 3.7 μm solar reflectance component. The green is brighter for smaller cloud particles. Therefore the polluted clouds with small drops appear yellow (see Areas 1, 5, and 6); whereas the ice clouds appear red (see areas 3 and 7). Pristine water clouds appear magenta (see Area 8), because they have low green (large water drops) and high blue (warm temperature). The line graphs provide the relations between the satellite indicated cloud top temperatures and the cloud top particle effective radii. At the foothills in Areas 1 and 5 the cloud top effective radius is much smaller than the precipitation threshold of 14 μm [*Rosenfeld and Gutman*, 1994] whereas the effective radius of 18 μm in Area 8 is much larger than the precipitation threshold.

trations reaching 1000 cm^{-3} over the southern Central Valley, including the location of Area 5 in Figure 12.

[41] The pristine clouds with large drops and warm rain processes produced a continuum of drop sizes from the cloud drops through the drizzle sizes to the small raindrops. In contrast, clouds with suppressed coalescence due to large CCN concentrations that grew to heights with cold temperatures still produced mixed phase precipitation mainly in the form of graupel. They produced distinctly different size distribution of the hydrometeors, which was separated from the cloud drop DSD. It is known from theoretical considerations and simulation studies that the decreased cloud drop sizes reduce also the mixed phase precipitation [*Khain et al.*, 2001; *Rosenfeld and Ulbrich*, 2003], but the extent of this possible effect from the cloud physics measurements remains to be documented.

[42] Similar response of clouds and precipitation forming processes to aerosols is apparent also in all the other research flights of SUPRECIP-2 as shown in the next subsection. The continued analyses and evaluation of the aircraft measurements provides compelling evidence for the detrimental role of anthropogenic aerosols on orographic precipitation in California, and explains how a climatological trend of increased CCN aerosols would cause the climatologically observed trends of the reduction in the orographic precipitation component in the southern and central Sierra Nevada.

3.1.2. Ensemble Results

[43] The next step was the analysis of all of the cloud passes on all the flights of SUPRECIP 2 to determine the cloud depth necessary for each cloud to develop particles of precipitation size as a function of the measured subcloud

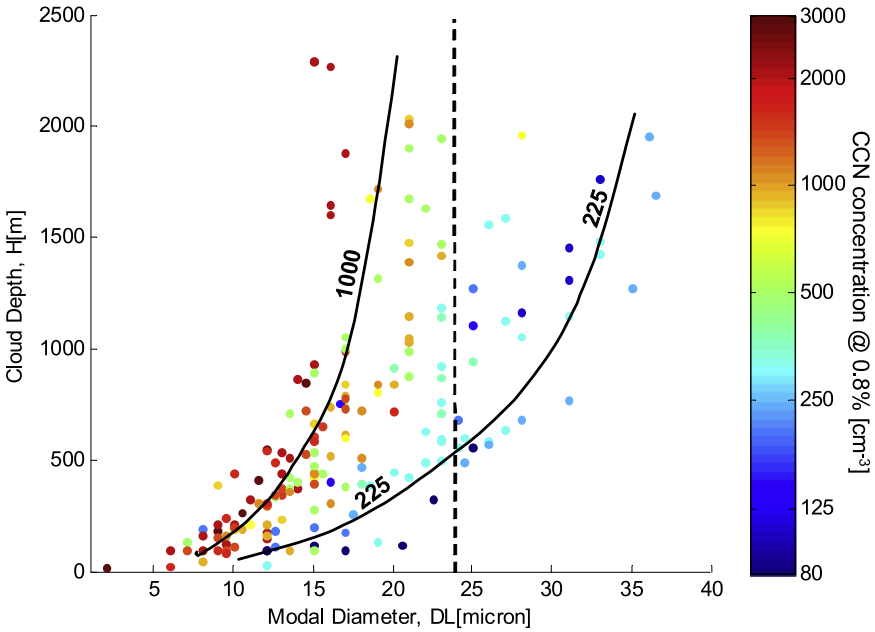

Figure 13. Scatterplot of the modal liquid water drop diameter (DL) versus the distance above cloud base height. Each plotted point has been colorized according to the scale on the right where browns, reds, and yellows indicate cloud passes with high subcloud CCN concentrations and blue points indicate cloud passes having low subcloud CCN concentrations. The vertical line marks the threshold for formation of precipitation-sized drops is when DL = 24 μm. The two lines are the approximated contours of 225 and 1000 CCN cm^{-3}, as done by the contouring routine of MATLAB. The contouring was done after transferring the individual data points to a surface by linear interpolation and initial smoothing.

CCN concentrations. This was done by determining the DL for each measurement. The dependence of DL on the CCN for all the measured clouds is provided in Figure 13. This parameter has been used elsewhere [*Andreae et al.*, 2004; *Rosenfeld et al.*, 2006] as shown in Figure 14 that gives the drop size for the modal LWC as a function of height for several regions and weather regimes around the world. The precipitation threshold was found to be D(LWC) = 24 μm [*Andreae et al.*, 2004] or DL24. From this diagram one can determine the typical cloud depths necessary for clouds to reach this precipitation threshold.

[44] The results of the analysis of the SUPRECIP 2 cloud passes are presented in Figure 13. Each dot on the figure represents the DL and its height above cloud base (H) for one cloud penetration. A cloud penetration was defined as a sequence of at least 3 s of CDP droplet concentration larger than 20 cm^{-3} and CDP LWC larger than 0.001 g/m^3. For each such penetration the average number of droplets in every size bin was calculated, and this gave the average size distribution for that penetration. Plotting the LWC density (for each bin normalized to the bin width) made it possible to derive the DL for each penetration manually. Only convective or cloud elements (mostly embedded) entered this analysis. Embedded small convective elements constituted much of the orographic clouds that formed at the foothills of the Sierra Nevada. Layer cap clouds dominated near the crest, but even they were mostly composed of embedded convection with elevated bases. Because of the uncertainty of cloud base height of these clouds, the clouds that were included in Figure 13 were formed mostly at the foothills and lower to midlevel western slopes of the Sierra Nevada.

[45] In order to be able to compare penetrations from different clouds and from different days, the cloud base height was subtracted from the penetration altitude to get the distance of the penetration from the cloud's base. The determination of the cloud's base is not always simple and straightforward because cloud base height can vary significantly even during a flight. Therefore in some cases the cloud base height needed to be adjusted so that the DL versus Cloud Depth (on a logarithmic scale) would fall approximately on a straight line (because the droplets grow very fast near cloud base and then at a decreasing rate thereafter (only when coalescence is not playing an important role). This uncertainty in the exact cloud base height leads to some uncertainty in the lowest parts of Figure 13.

[46] Last, the color of each small circle is determined by the measured (by the aerosol aircraft) CCN concentration in the vicinity and below the bases of the penetrated clouds at the maximum supersaturation of ~0.85%. The scale of the coloring is logarithmic in order to increase the definition/resolution at low CCN concentrations.

[47] Figure 13 shows that the difference in DL between clouds developing in polluted air (high CCN concentrations) and clouds developing in clean air becomes more and more pronounced with height. The DL of polluted clouds having high CCN concentrations is significantly smaller higher in the clouds, because it increases more slowly with cloud depth than in clouds with low CCN concentrations. The clouds need to be deep enough and the DL needs to

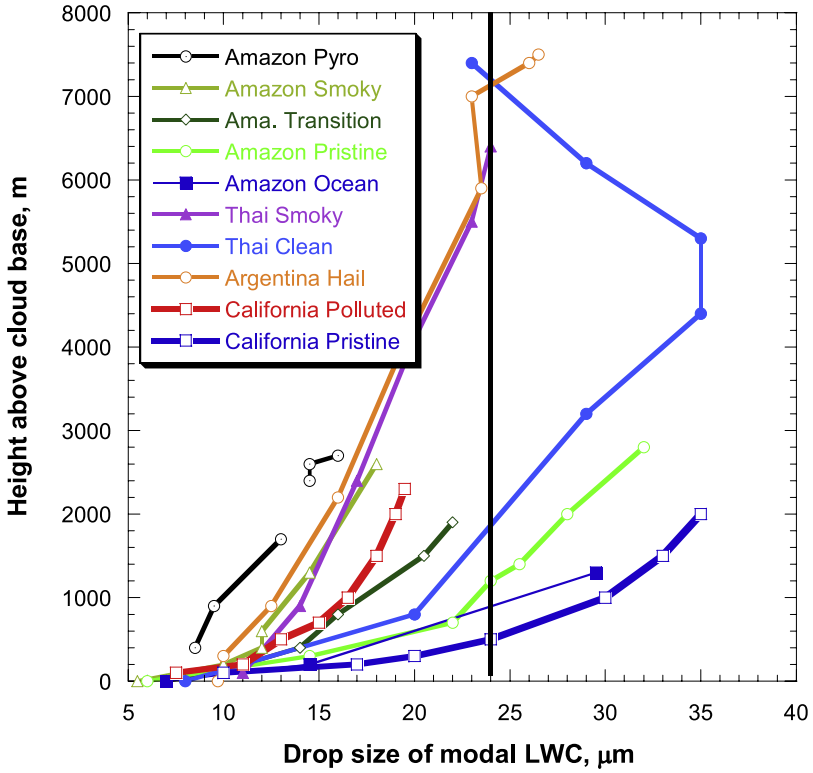

Figure 14. The global context of the dependence of the drop size modal LWC DL on height above cloud base and temperature. The lines, according to their order in the legend, are: Amazon pyro-Cb, smoky, transition, pristine over land and pristine over ocean clouds [*Andreae et al.*, 2004]; Thailand premonsoon smoky and monsoon relatively clean clouds [*Andreae et al.*, 2004]; Argentina microphysically continental hail storms [*Rosenfeld et al.*, 2006]; California polluted and pristine clouds [Figure 13 of this study). The vertical line at DL = 24 μm represents the warm rain threshold.

reach ~24 μm before significant warm rain can occur. Therefore the differences in the (warm) precipitation processes become larger higher in the clouds, at least up to 2–2.5 km above their bases, which was reached by the cloud physics aircraft. Because deeper clouds have a greater potential to precipitate large amounts of water, this figure indicates that the aerosols influence the precipitation amounts from these clouds. This serves as evidence of the direct connection between pollution aerosols and the suppression of precipitation at least in the winter shallow convective and orographic clouds in Central California.

[48] Again, Figure 14 shows the global context of the height-DL relations found for pristine and polluted clouds in the study area. According to Figure 14, the pristine clouds in California precipitated at heights starting at 0.5 km, shallower than in the pristine tropical clouds. The polluted clouds in California had larger drops than the respective smoky clouds in the Amazon and Thailand, reflecting the much greater concentration of smoke CCN there than exist currently in the California air pollution during rainy days. This means that the precipitation in these California clouds could be suppressed further if the air pollution concentrations become even greater.

3.2. Diurnal Variability of the Aerosols

[49] All of the analyses to this point indicate that the ingested aerosols determine cloud internal structure, either promoting or suppressing the formation of precipitation. There are very strong indications that anthropogenic aerosols generated within California act to decrease the droplet sizes and suppress coalescence processes and precipitation, especially in Sierra orographic clouds. To understand these processes it is important to document the evolution of these aerosols and their effects on clouds during the diurnal cycle. There was an opportunity to do this on 2 March 2006 when three flights were conducted by each of the research aircraft. Their flight tracks are shown in Figure 15. Note that the aerosol aircraft stayed close to Sacramento on all three flights because of the showery weather, flying according to visual flight rules (VFR) in ascending and descending orbits from roughly 1,000 to 10,000 ft. The cloud physics aircraft had no such VFR restrictions and flew the tracks as shown.

[50] Figure 16 shows plots versus height of the CN (total aerosols) and CCN (raw and adjusted to 0.9% supersaturation) concentrations in cm^{-3} measured by the aerosol aircraft on the three flights of 2 March 2006 (top three panels) and the corresponding plots as a function of height of the droplet concentrations and sizes (r_e) measured by the cloud physics aircraft on its three flights of the day (lower three panels).

[51] Beginning with the top three aerosol plots, it is evident that the aerosol concentrations are highest at the low levels in the morning. By the late morning and afternoon, however, the aerosol concentrations have decreased substantially at low levels while increasing above as convective currents carry the aerosols to higher altitudes.

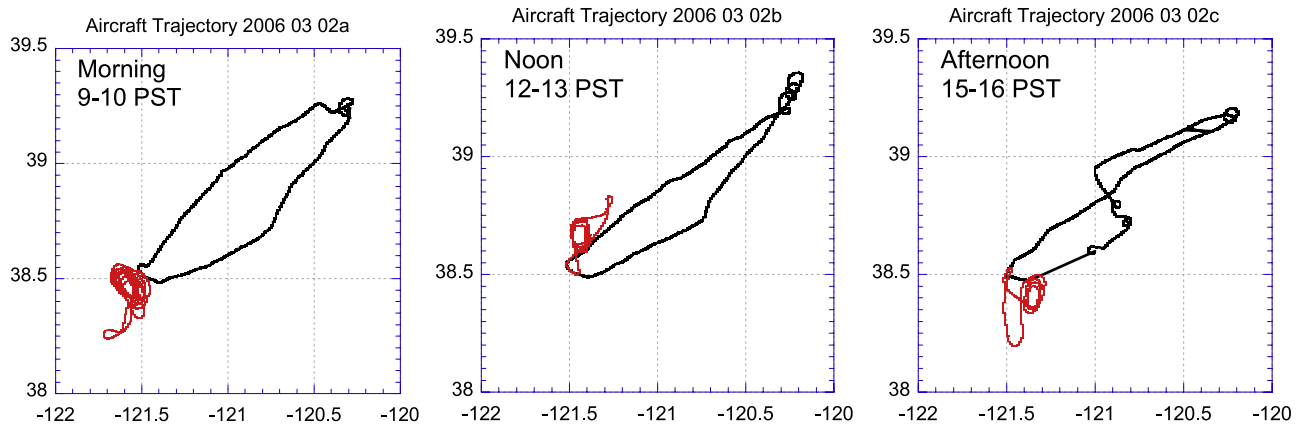

Figure 15. The flight tracks for the aerosol (red) and cloud physics (black) aircraft for the three flights on 2 March 2006.

Thus the aerosols at an elevated altitude should show a strong diurnal cycle. Indeed this was the case on this day as shown in Figure 17 for the Blodgett Forest Research Station (at an elevation of 1314 m) where aerosol measurements were made throughout SUPRECIP 2 by Desert Research Institute (DRI) CCN spectrometers [*Hudson*, 1989] and a TSI 3010 CN counter. In referring to the Blodgett aerosol plots in Figure 17 note that there is a gap in the data during the middle of the day due to a power failure. Even so, a strong diurnal cycle is evident in the plots. The measurement flights of the day took place between 09:00 and 16:15 PST. Fortunately, some aerosol data were collected during the flight period despite the substantial data gap. At noon local time (1200 PST) the CCN at 1% S and CN concentrations measured by the aerosol aircraft at the altitude of the Blodgett station but over 100 km distant to the southwest were roughly 220 and 1700 particles/cc, respectively. At Blodgett itself the CCN and CN measurements at noon just before the data stream ended were 600 and 1200 particles/cc, respectively. This is reasonable agreement when one considers the physical distance between the Blodgett site and the orbiting aircraft at this time on 2 March 2006.

[52] Referring back to Figure 16 for the plots of cloud droplet concentrations and r_e from the observations of the cloud physics aircraft (bottom three panels), it can be seen that the changes in the droplet measurements were associated with the changes in the aerosols. With respect to the morning flight, the droplet concentrations were highest (up to 800/cc) and their sizes were smallest (<9 μm) near the cloud base of 500 m. (In order to obtain the effective radii sizes, divide the abscissa scale by 100.) Above 1000 m, however, the drop concentrations were <200/cc and the r_e were as high as 16 μm. By the midday flight the cloud bases had risen to 800 m where the CCN aerosol concentrations reached as high as 1000/cc. The changes were greatest for the afternoon flight (lower right panel). By this time cloud base was just above 1000 m, the CCN concentrations had increased to 500/cc over a considerable depth (about 2000 m) above cloud base and the droplet sizes were much smaller (mostly <10 μm diameter) between cloud base and 5000 m altitude. The changes were quite appreciable relative to what was measured during the morning flight. The low-level aerosols had clearly been transported upward, increasing the droplet concentrations with height and decreasing their sizes in clouds that had ingested them.

[53] The diurnal changes in aerosol concentrations that were documented by aircraft on 2 March 2006 are typical for the region as is shown in the February and March 2006 mean CN and CCN aerosol plots versus time at the Blodgett Research Station (Figure 18). Note that the amplitude of the aerosol oscillation at Blodgett is about a factor of two for the CN and CCN aerosols with the minimum and maximum concentrations in both months occurring at 0700 PST and 1900 PST, respectively. The counts were higher in February than in March 2006 because it was the drier and "dirtier" of the 2 months.

[54] The plots of the aerosols on 2 March 2006 suggest that they originate at the Earth's surface and that they are transported upward by convective currents during the day. This is why the maximum aerosol concentrations are not reached at Blodgett until late in the afternoon. It also means that the greatest suppressive effect of aerosols on clouds will take place late in the day and the subsequent evening when the cumulative heating will produce the convective currents necessary to carry the pollution aerosols into the clouds. Assuming that the physics is correct, the maximum suppressive effect of aerosols should be most noticeable in spring storms when the sun is stronger, the heating is greater, the resulting convective currents are stronger, and the photochemical processes leading to the formation of aerosols are most active.

[55] This hypothesis was tested by examining the precipitation records at two paired (mountain versus valley) sites, first at Cuyamaca, a mountain station to the east northeast of San Diego, versus the precipitation record at San Diego itself. These paired stations were chosen because of their long, high-quality precipitation records that extend back to 1885. These stations also figured prominently in the paper by *Givati and Rosenfeld* [2004] in which they laid out their analysis methods. In this instance the analysis of the orographic enhancement factor was done separately for the fall (November through January) and spring (February through April) months in each year. The usual scatterplot with best fit lines of the orographic factor for fall and spring is provided in the left panel of Figure 19. Note that, as

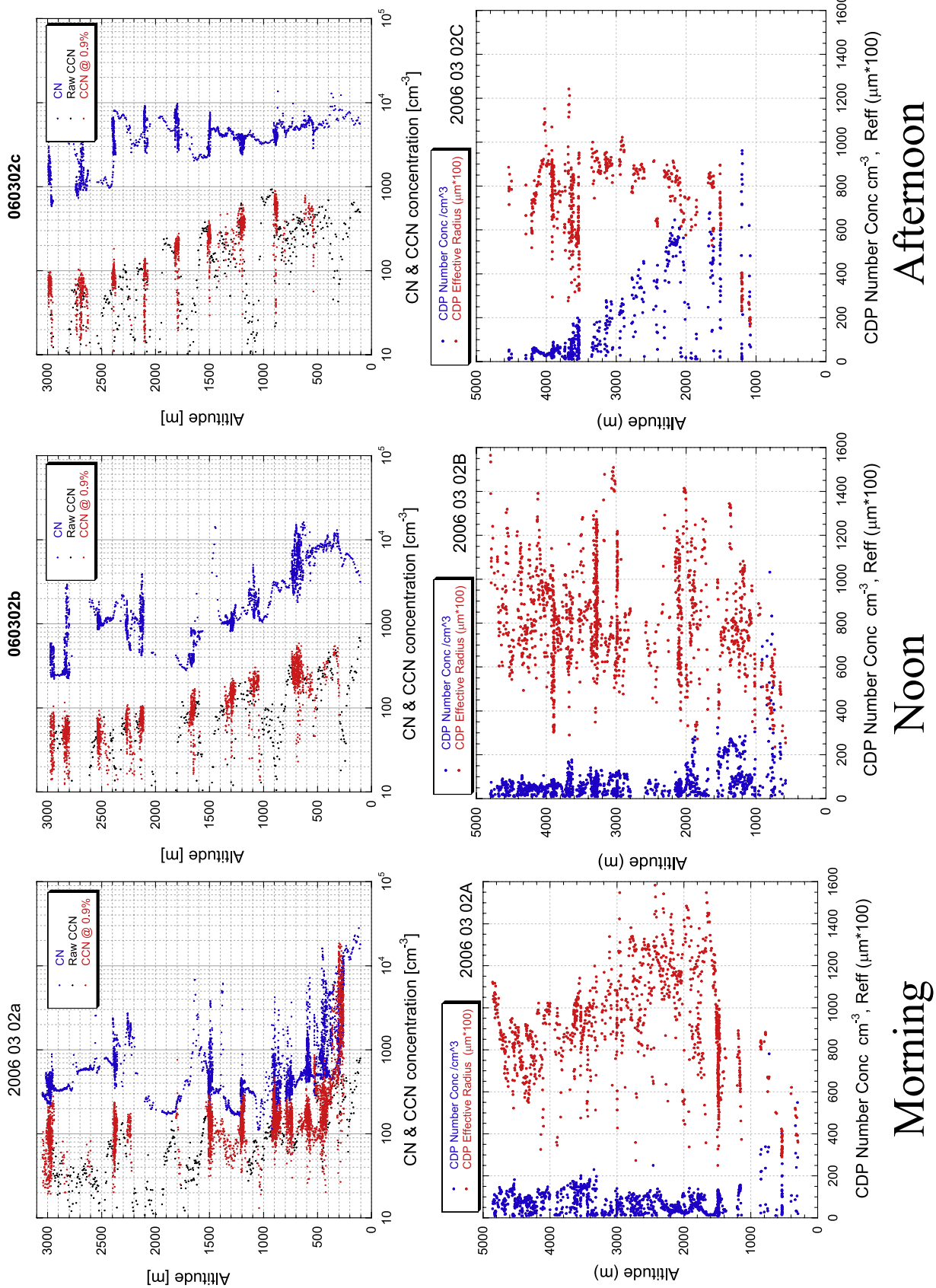
Morning
Noon
Afternoon
2006 03 02a
060302b
060302c
2006 03 02A
2006 03 02B
2006 03 02C
CN
Raw CCN
CCN @ 0.9%
CDP Number Conc /cm^3
CDP Effective Radius (µm*100)
Altitude [m]
Altitude (m)
CN & CCN concentration [cm^-3]
CDP Number Conc cm^-3, Reff (µm*100)

Figure 16

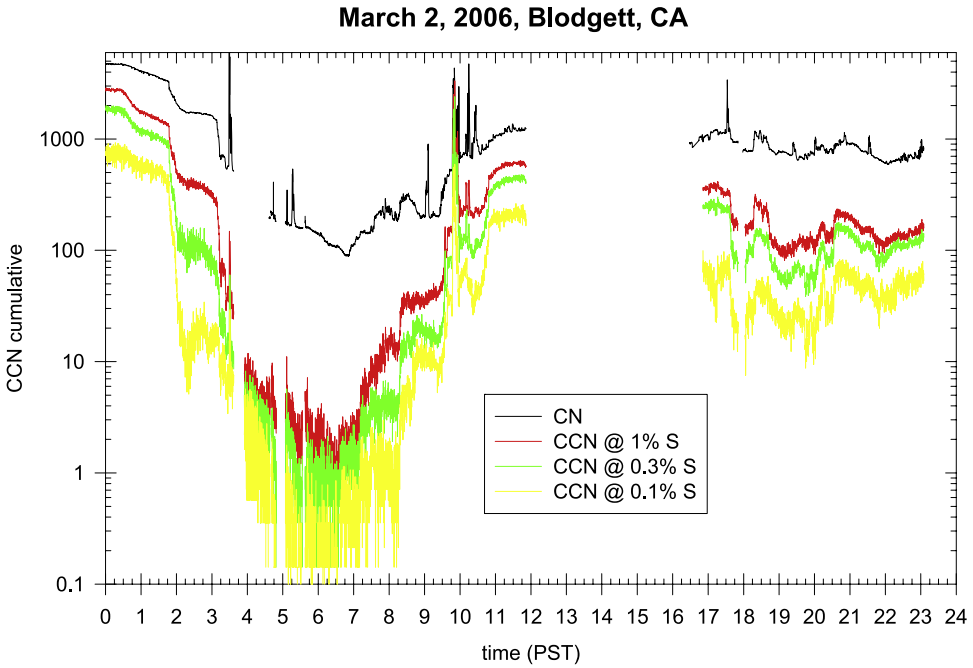

Figure 17. Plots of the CCN (at three supersaturations) by the DRI instrument [*Hudson*, 1989] and CN aerosols observed at the Blodgett Forest Research Station (1314 m elevation) on 2 March 2006. Despite a gap in the data stream, a strong diurnal cycle is evident in the plots. The measurement flights of the day took place between 09:00 and 16:15 PST.

predicted, the loss of orographic precipitation at Cuyamaca in the spring (−29%) is nearly twice the precipitation loss in the fall (−15%). The second paired stations were gages at Placerville in the Sierra Mountains versus Sacramento in the Sacramento Valley. The same pattern is evident with the stronger decrease in the orographic enhancement factor Ro evident in the spring (−27%) than in the fall (−17%). Here again, additional pieces of the puzzle have fallen into place identifying anthropogenic aerosols for the suppression of orographic precipitation in the California Sierra Nevada.

3.3. Spatial Distribution of the Aerosols

[56] The spatial distribution of condensation nuclei (CN) and those aerosols that acted as cloud condensation nuclei (CCN) at supersaturations up to 0.9% was of great interest in SUPRECIP 2. By compositing all of the flights of the aerosol aircraft it was hoped that an informative pattern would emerge as a function of space, time, altitude and wind regime. The first step of the analysis was a print out of the adjusted CCN observations made by the aerosol aircraft on all flights when it was flying below 5000 ft as shown in Figure 20. The boundary layer winds were not considered in making this plot. The observations were color-coded along the track. The portions of the track that are orange to brown had CCN concentrations >1000 particles/cc while those portions that have light blue to dark blue coloration had CCN concentrations <100 particles/cc. The pattern proved to be somewhat of a surprise because the highest CCN concentrations were found in the Central Valley, mostly to the east and south of Sacramento and not so much in the coastal urban areas as had been expected. Although high counts had been experienced intermittently in the San Francisco/Oakland areas, the high counts farther south in the Central Valley cannot be explained as readily by the simple transport of pollutants from the west. This suggests the possibility of significant generation of pollutants in the Central Valley itself. These findings are consistent with those published by *Chow et al.* [2006] resulting from the analysis of an extensive surface-measurement program for the measurement of aerosol concentrations and their chemistry in this region.

[57] The next step was the compositing of the flights that had similar boundary layer winds, because the movement of the aerosols obviously depends on the low level winds. Streamline maps for the surface winds were obtained from NOAA's Air Resources Laboratory for each flight day. An example of the streamline map for the afternoon flight on 28 February 2006 (already 00Z on 1 March 2007),

Figure 16. Plots as a function of height (in meters) of the CN (total) and CCN concentrations (cm^{-3}) measured by the aerosol aircraft on the three flights of 2 March 2006, during its step-climb to 3 km altitude (top) and the corresponding plots as a function of height (in meters) of the droplet concentrations and sizes (effective radius) measured by the cloud physics aircraft on its three flights of the day (bottom). The red dots in the top show the adjusted CCN measurements (to 0.9% supersaturation) only during horizontal flight (ascent rate $<\pm 3$ m/s). This was done to take into account the varying supersaturations (in the range of ~0.1−0.85%) and because decreases in the raw CCN concentrations were noted while the aircraft was ascending. The black dots are the raw CCN measurements.

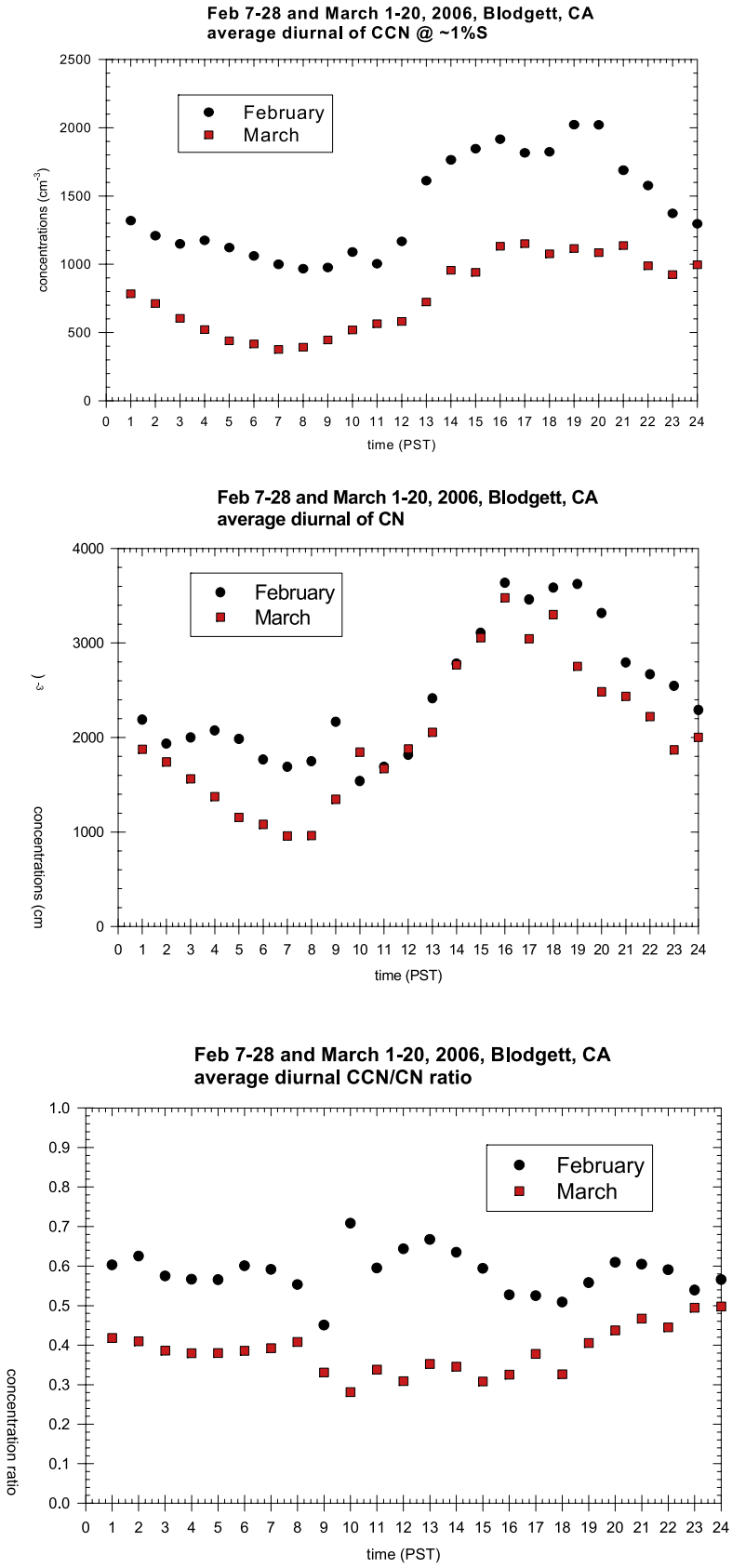

Figure 18. Mean time (PST) plots for February (black) and for March (red) 2006 of the CCN (top) and CN total aerosol (middle) concentrations measured at the Blodgett Research Station by the DRI CCN instrument. Plots of the ratio CCN/CN in February (black) and March (red) are given in the bottom panel. The CCN aerosol measurements were made at a supersaturation of 1%.

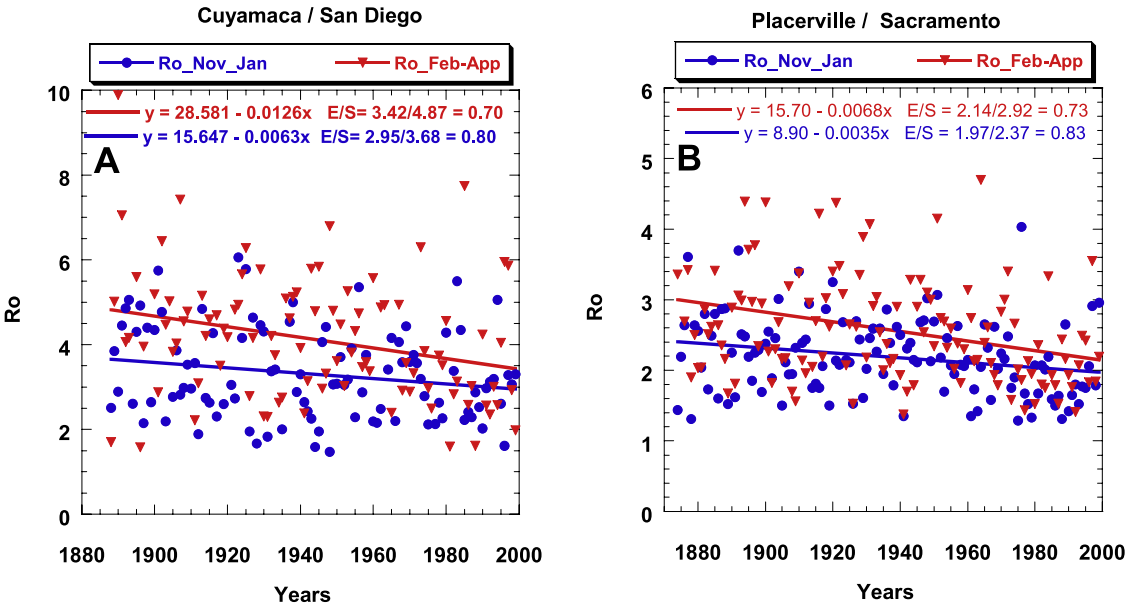

Figure 19. Scatterplot of the orographic precipitation enhancement factor (Ro) in the fall and spring for the years 1885 to 2000 for Cuyamaca versus San Diego (panel A) where Ro is defined as the ratio of the precipitation at the mountain station (Cuyamaca) to the precipitation at the upwind lowland plains or coastal station. Panel B shows the same for Ro between a mountain gauge cluster near Placerville versus a cluster at the Sacramento area. The apparent effect of pollution on precipitation at the mountain station is obtained by taking the ratio of Ro at the end of the period of interest to Ro at the outset of the period, where the ending and starting Ro values are obtained from the best fit line to the scatterplot. In this instance the analysis was done separately for the fall and spring months. Although precipitation losses occurred in both the fall and spring, the losses were greater in the spring (i.e., −27 to −30%) than in the fall months (i.e., −17% to −20%) because the sun is stronger in the spring months during which convective currents would more readily transport pollution aerosols to higher altitudes.

the flight that was discussed extensively earlier is provided in Figure 21.

[58] The CCN plots partitioned by wind direction were not any more informative than the overall plot in Figure 20, because there was not that much variability in wind direction on the flight days. The plot for southwesterly winds is given in Figure 22 for flights at <5000 ft. The plot is similar to that in Figure 20 without wind partitioning. The rest of the wind-partitioned plots were not any more informative because of the rather small sample.

[59] The total aerosol plots of condensation nuclei (CN) are also of considerable interest. The overall plots for all flights without wind partitioning are given in Figure 23. Not surprisingly, it bears a strong resemblance to the overall CCN plots, except in this case the counts are much higher, especially in the central and eastern portions of the Central Valley as is the case with the overall CCN plots. With such a heavy aerosol loading it comes as no surprise that this is the area in the Sierra where the suppression of precipitation and runoff is greatest.

[60] It is informative to look at plots of the ratio of CCN to CN to determine what fraction of the total aerosol serves as CCN. This is done in Figure 24 for all flights when the aerosol aircraft was flying at an altitude <5000 ft. Although there are exceptions, the CCN/CN ratio ranges from 0.1 to 0.2 over most of the map. This is considerably smaller than the mean ratio documented at the Blodgett aerosol site at which the mean ratio CCN/CN was about 0.6 in February and 0.4 in March (see Figure 18). The reason(s) for the differing mean ratios is unknown. It may be due to CN concentrations closer to their sources, since the CN tend to decrease farther from their immediate sources.

4. Discussion

[61] The pieces of the research puzzle are slowly falling into place with respect to the trend of decreasing orographic precipitation over many areas of the globe and attendant losses in runoff [*Woodley Weather Consultants*, 2007] and spring flows [*Rosenfeld et al.*, 2007]. With respect to California it was determined also that the Pacific decadal oscillation (PDO) and the Southern Oscillation index (SOI) [*Allan et al.*, 1991; *Dettinger et al.*, 2004], cannot explain the observed declining trends in the orographic enhancement factor (Ro) [*Rosenfeld and Givati*, 2006].

[62] These apparent losses in orographic precipitation are not limited to California. *Rosenfeld and Givati* [2006] expanded their study to the whole western USA, where they showed that Ro remained stable over hills in the more pristine areas in northern California and Oregon, but decreased again to the east of the densely populated and industrialized Seattle area. Similar effects were observed not only in the Pacific coastal areas, but also well inland. Precipitation was decreased by 18% over the mountains to the east of Salk Lake City, Utah, but remained unchanged at the southern extension of the same mountain range

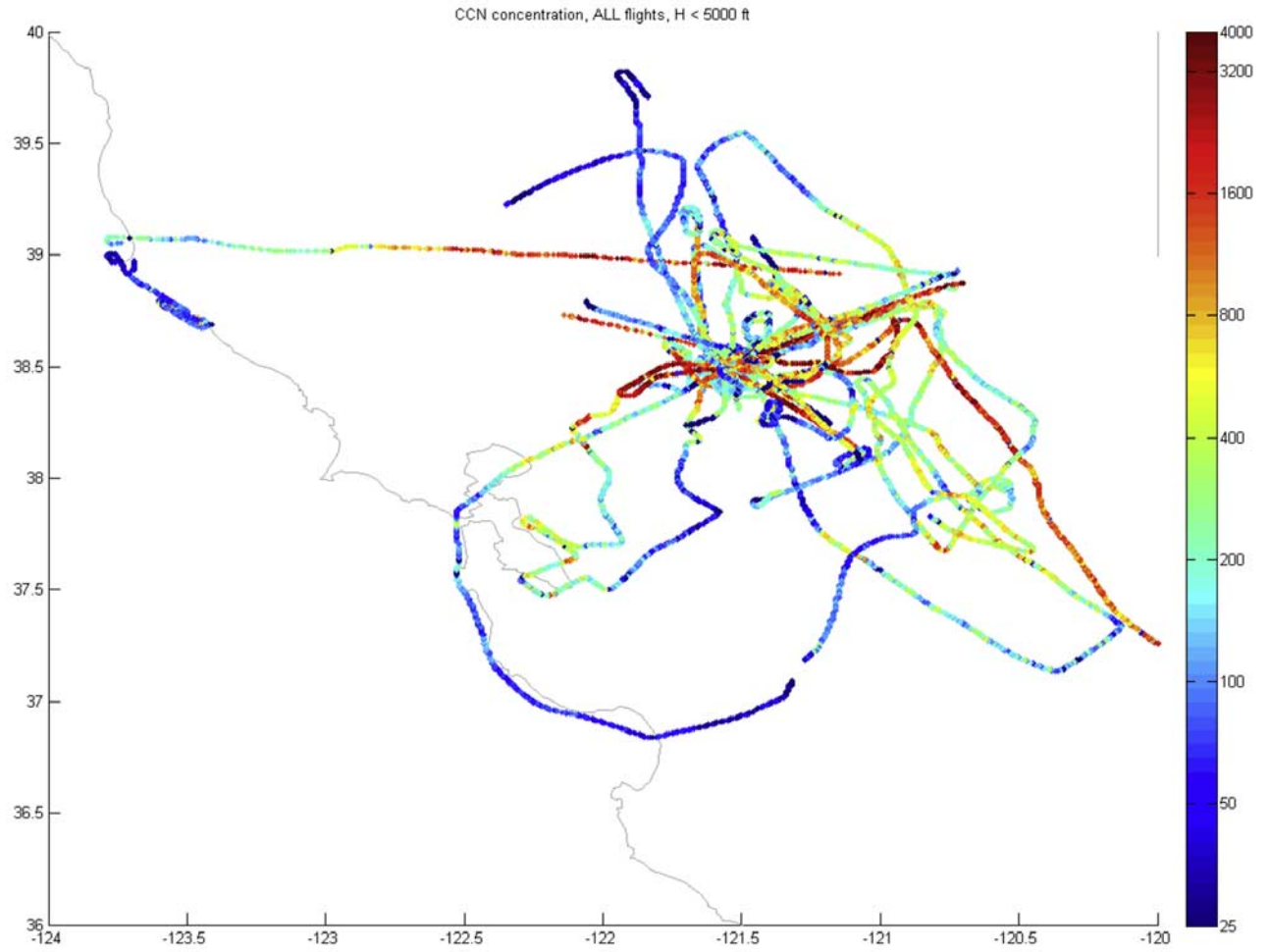

Figure 20. A colorized plot summary of the CCN measurements made on all flight days without wind partitioning during SUPRECIP 2 when the aerosol aircraft was flying below 5000 ft, almost exclusively below cloud base. According to the legend, the portions of the track when the CCN readings exceeded 1000/cm^3 are orange changing to dark brown at readings of 4000/cm^3. The portions of the track when the CCN readings were <100/cm^3 begin at light blue and change to dark blue for the lowest CCN concentrations. Note that the highest CCN readings were in the Sacramento area and south-eastward to the Sierra foothills.

[*Rosenfeld and Givati*, 2006; *Griffith et al.*, 2005]. Similar effects were found during easterly winds over the eastern slope of the Rocky Mountains downwind (i.e., to the west) of Denver and Colorado Springs [*Jirak and Cotton*, 2006].

[63] The common denominator for the regions suffering losses in orographic precipitation has been found in the multispectral satellite imagery that shows decreased cloud-particle (r_e) for the affected regions. In California this was addressed using multispectral satellite images from polar-orbiting satellites [*Woodley Weather Consultants*, 2007]. On each day with a satellite overpass, the multispectral imagery was processed to infer the r_e of cloud particles for the clouds within selected areas within the field of view. This was done because previous studies had shown that areas with small r_e are slow to develop precipitation. After the satellite inferences had been made they were composited geographically. It was found that r_e increases more slowly with decreasing T in the central and southern Sierra compared to the northern Sierra. The slower increase of r_e with elevation is the most robust indicator for the slower development with height of precipitation in the clouds. This finding is consistent with the gauge and streamflow analyses that show that the greatest losses of water occur in the central and southern Sierra [*Woodley Weather Consultants*, 2007]. This suggested a major role of CCN pollutants that are ingested by the orographic clouds with consequent suppression of coalescence along the lines of the hypothesis put forth at the outset of this paper.

[64] SUPRECIP was designed to address the potential linkages between pollution aerosols and the loss of orographic precipitation and subsequent runoff. SUPRECIP 1 showed a strong positive correlation between the satellite-inferred cloud microphysics and the aircraft-measured cloud microphysics. Thus the areas in the central and southern Sierra that were shown by satellite to have smaller r_e than

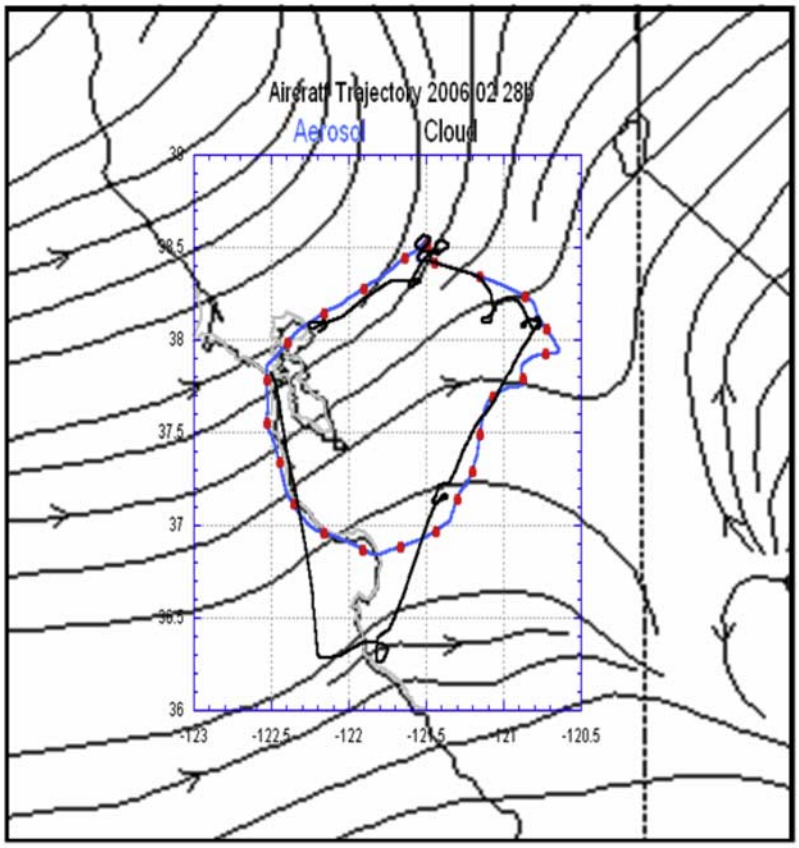

Figure 21. Surface streamline map for Central and Northern California at 00 UTC on 1 March 2006 produced by the Air Resources Laboratory of NOAA. The flight tracks of the cloud physics (black) and aerosol aircraft (blue with red dots every 5 min along the track) have been superimposed on the streamline presentation. The flight tracks are the same as those presented earlier in Figure 6.

over the northern Sierra likely really do have suppressed precipitation forming processes.

[65] It took SUPRECIP 2 to make this direct connection between the pollution aerosols and suppressed precipitation-forming processes. The scatterplot of the modal liquid water drop diameter (DL) versus the depth above cloud base height (Figure 13) as a function of the ingested CCN shows that clouds growing in a polluted environment must reach greater depths to develop precipitation than clouds growing in a more pristine environment where the CCN concentrations are lower.

[66] In looking at the temporal and spatial patterning of the pollution aerosols in California, it was determined that they typically exhibit a strong diurnal oscillation with the strongest upward transport during the late afternoon. Thus the sampled clouds are more continental in character with smaller droplet sizes and diminished coalescence at this time of day. The aerosol concentrations were minimal over the sea and increased after traversing the shoreline, where urban and industrial development has taken place. The aerosols found over the Central Valley were not simply transported from the coastal areas, because on most days the CN and CCN concentrations in the Valley to the Sierra foothills exceeded what was found in the coastal urbanized areas. This is true especially in the central and southern Valley well to the east of sparsely populated coastal regions. This is consistent with slow gas to particle conversion and aging by coagulation of aerosol to form CCN. It appears, therefore, that the large aerosol concentrations that are likely suppressing the Sierra orographic precipitation are generated locally in the Valley itself having unknown specific origins and chemistry. This is consistent with the findings of *Chow et al.* [2006] from an extensive aerosol measurement program in the San Joaquin Valley. Although transport of pollution aerosols from the sea and from coastal regions may play a role in the suppression of Sierra orographic precipitation, it would appear to be secondary to the role being played by the local generation of aerosols in regions of highest concentrations. Understanding this role would appear to be the next logical step in this research effort.

[67] A major component of this research effort was model simulation of the effects of aerosols [*Lynn et al.*, 2007]. The simulation with clean air produced more precipitation on the upwind mountain slope than the simulation with continental aerosols. After 3 h of simulation time, the simulation with maritime aerosols produced about 30% more precipitation over the length of the mountain slope than the simulation with continental aerosols. Greater differences in precipitation amounts between simulations with clean and dirty air

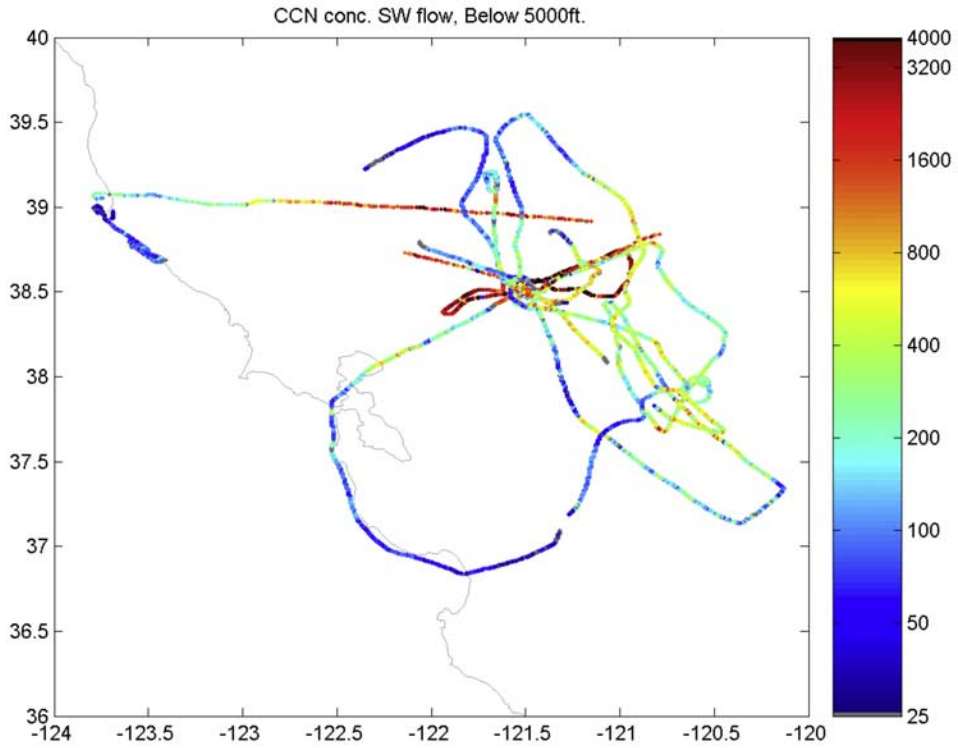

Figure 22. The same as for Figure 20 but for southwesterly surface wind flows.

were obtained when ice microphysical processes were included in the model simulations.

[68] Thus the totality of the evidence from the research effort, involving precipitation and streamflow analyses, quantitative satellite measurements, numerical modeling and extensive aircraft measurements of cloud properties and aerosols, makes a strong case for the loss of precipitation and stream flows in the California Sierra Nevada due to

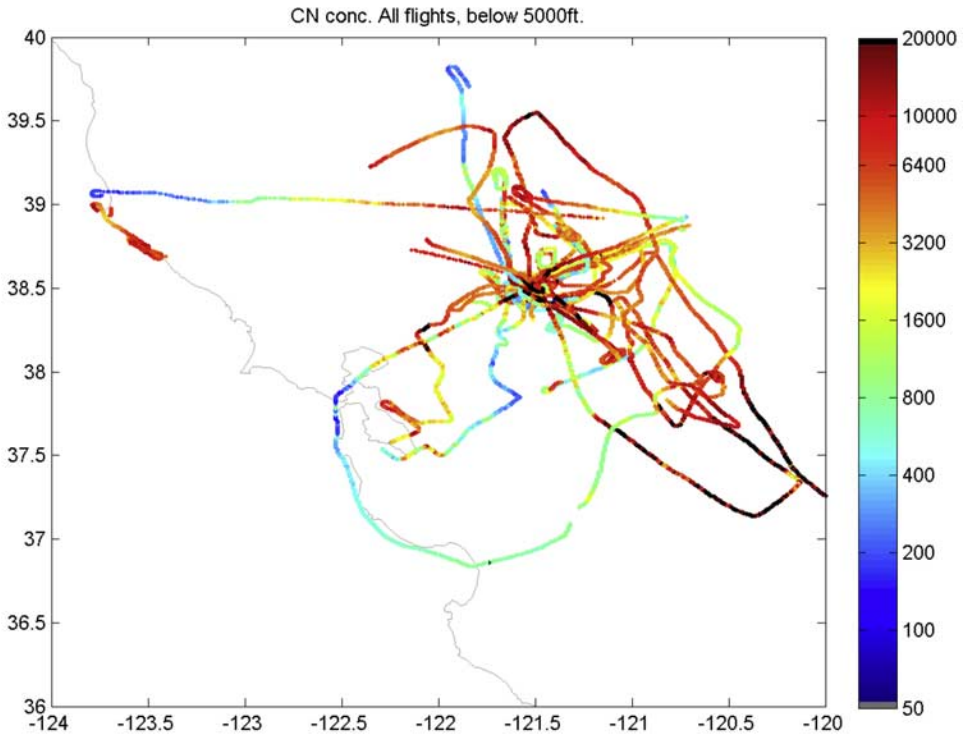

Figure 23. The same as in Figure 20, but for the CN (total aerosols) measurements.

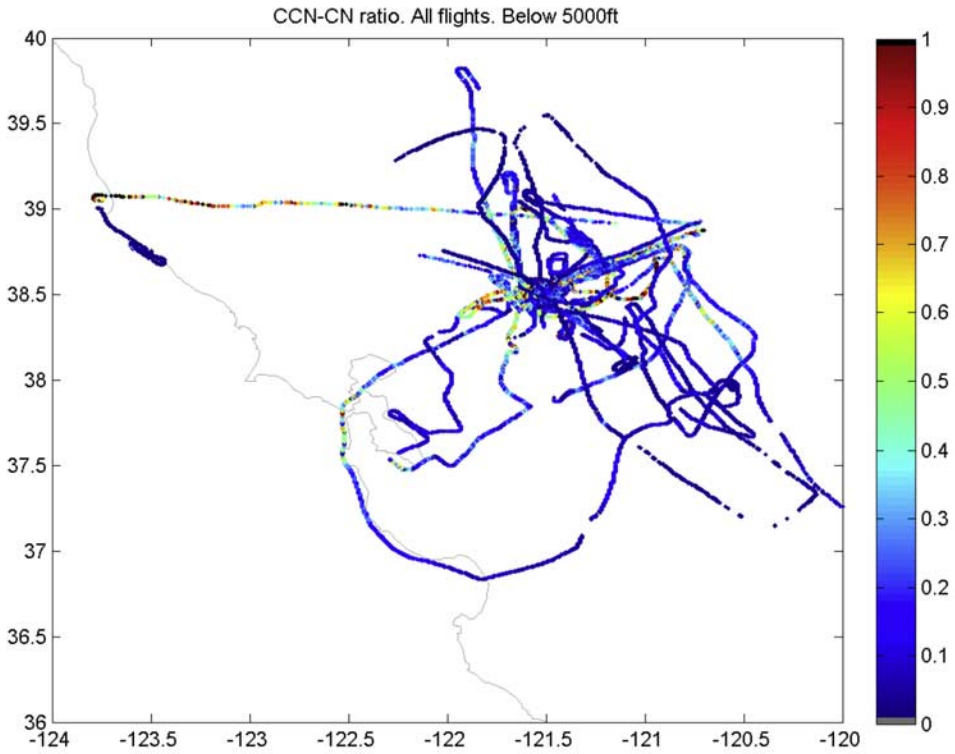

Figure 24. The same as for Figure 20 but for the ratio of CCN to CN. The colorized portion of the track can be related to CCN/CN from the figure legend.

the generation of anthropogenic pollutants and their ingestion into Sierra clouds.

5. Conclusions

[69] SUPRECIP 2 met its primary objective of documenting the effects of pollution aerosols on clouds and their precipitation over the California Sierra Nevada. The aircraft measurements of cloud properties validated the satellite inferences of cloud microphysics. Those regions over which the processed multispectral imagery indicated the clouds had small droplet sizes and suppressed coalescence versus those areas where the satellite inferences indicated the clouds had large droplet sizes and coalescence were verified by the aircraft measurements. This makes the satellite inferences of altered cloud properties in the central and southern Sierra all the more credible.

[70] The key uncertainty at the outset of SUPRECIP was whether the altered cloud properties were due to the ingestion of pollution aerosols. Although SUPRECIP 1 gave the first indications of a link between the pollution aerosols and the suppression of precipitation-forming processes, it took SUPRECIP 2 utilizing two cloud physics aircraft to demonstrate the direct linkage between these aerosols and the regions in the central and southern Sierra Nevada that have suffered losses of orographic precipitation and stream flows. The analysis of several hundred cloud passes shows that in regions where high concentrations of CCN were measured by the base aerosol aircraft the clouds had to grow to greater depths to develop precipitation than clouds growing in regions of low CCN concentrations.

[71] The spatial and temporal documentation of the CCN and CN aerosols was highly informative. Although the initial source of the pollution aerosols was clearly the urbanized coastal regions, the pollution aerosols in the Central Valley to the Sierra foothills cannot be explained readily by simple advection of the pollutants from the coastal urban areas. There is probably a major source of pollution aerosols in the Central Valley itself and these CCN and total (CN) aerosols are concentrated primarily over the Central Valley from just to the north of Sacramento southward along the foothills to south of Fresno. This is the same region that has been shown through statistical analysis of precipitation and streamflow records to suffer the greatest loss of winter orographic precipitation and subsequent stream flows.

[72] The pollution aerosols show a strong diurnal oscillation. In the morning these aerosols are concentrated at low levels, but by late afternoon they have been transported upward due to the afternoon heating. Thus the regional clouds are most affected by the pollutants late in the day. The aircraft measurements indicate that the ratio of CCN to CN (total) aerosols is typically 0.10 to 0.20 whereas the measurements at the ground-based (Blodgett) site indicate that the ratios are higher.

[73] Because the local generation of the pollution aerosols in the Central Valley appears to be a greater problem than the transport of pollution from the urbanized/industrialized coastal regions or inland from the Pacific, the next step in the research progression is to document the sources and chemical constituency of the aerosols in the Central Valley. The evidence amassed from SUPRECIP and the ancillary

precursor research conducted by the authors indicates that the precipitation and streamflow losses are real and due primarily to the ingestion of pollutants by orographic clouds over the Sierra Nevada. Further, the results of model simulations demonstrating the detrimental effects of pollutants on Sierra orographic precipitation give additional weight to the hypothesis put forth at the outset of this paper.

[74] **Acknowledgments.** The authors gratefully acknowledge the major contributions that the pilots made to the success of the SUPRECIP field effort. David Prentice piloted the Cheyenne II cloud physics aircraft during SUPRECIP 1 and Gary Walker, Manager of the SOAR program of the Sandyland Underground Water Conservation District piloted this aircraft in SUPRECIP 2. Kevin McLaughlin piloted the Cessna 340 aerosol aircraft. The authors also acknowledge Don Collins and Crystal Reed of Texas A&M University for their support with the DMA/TDMA system and Ing. Grazio Axisa for maintaining the aircraft instruments in SUPRECIP 2. The research was supported by the Public Interest Energy Research (PIER) program of the California Energy Commission (CEC). We especially appreciate the enthusiastic encouragement of Guido Franco of PIER/CEC throughout the research effort.

References

Allan, R. J., N. Nicholls, P. D. Jones, and I. J. Butterworth (1991), A further extension of the Tahiti-Darwin SOI, early SOI results and Darwin pressure, *J. Clim.*, *4*, 743–749.

Andreae, M. O., D. Rosenfeld, P. Artaxo, A. A. Costa, G. P. Frank, K. M. Longo, and M. A. F. Silva-Dias (2004), Smoking rain clouds over the Amazon, *Science*, *303*, 1337–1342.

Borys, R. D., D. H. Lowenthal, and D. L. Mitchell (2000), The relationships among cloud microphysics, chemistry and precipitation rate in cold mountain clouds, *Atmos. Environ.*, *34*, 2593–2602.

Borys, R. D., D. H. Lowenthal, S. A. Cohn, and W. O. J. Brown (2003), Mountaintop and radar measurements of anthropogenic aerosol effects on snow growth and snowfall rate, *Geophys. Res. Lett.*, *30*(10), 1538, doi:10.1029/2002GL016855.

Chow, J. S., L.-W. A. Chen, J. G. Watson, D. H. Lowenthal, K. A. Magliano, K. T. Turkiewicz, and D. E. Lehrman (2006), $PM_{2.5}$ chemical composition and spatiotemporal variability during the California Regional $PM_{10}/PM_{2.5}$ Air Quality Study (CRPPAQS), *J. Geophys. Res.*, *111*, D10S04, doi:10.1029/2005JD006457.

Dettinger, M., K. Redmond, and D. Cayan (2004), Winter orographic precipitation ratios in the Sierra Nevada – Large-scale atmospheric circluations and hydrologic consequences, *J. Hydrometeorol.*, *5*, 1102–1116.

Gerber, H. (1996), Microphysics of marine stratocumulus clouds with two drizzle modes, *J. Atmos. Sci.*, *53*, 1649–1662.

Givati, A., and D. Rosenfeld (2004), Quantifying precipitation suppression due to air Pollution, *J. Appl. Meteorol.*, *43*, 1038–1056.

Givati, A., and D. Rosenfeld (2005), Separation between Cloud Seeding and Air Pollution Effects, *J. Appl. Meteorol.*, *44*, 1298–1314.

Givati, A., and D. Rosenfeld (2007), Possible impacts of anthropogenic aerosols on water resources of the Jordan River and the Sea of Galilee, *Water Resour. Res.*, *43*, W10419, doi:10.1029/2006WR005771.

Griffith, D. A., M. E. Solak, and D. P. Yorty (2005), Is air pollution impacting winter orograhic precipitation in Utah? Weather Modification Association, *J. Weather Modif.*, *37*, 14–20.

Hudson, J. G. (1989), An instantaneous CCN spectrometer, *J. Atmos. Oceanic. Technol.*, *6*, 1055–1065.

Hudson, J. G., and S. Mishra (2007), Relationships between CCN and cloud microphysics variations in clean maritime air, *Geophys. Res. Lett.*, *34*, L16804, doi:10.1029/2007GL030044.

Hudson, J. G., and S. S. Yum (2001), Maritime-continental drizzle contrasts in small cumuli, *J. Atmos. Sci.*, *58*, 915–926.

Jirak, I. L., and W. R. Cotton (2006), Effect of air pollution on precipitation along the Front Range of the Rocky Mountains, *J. Appl. Meteorol.*, *45*, 236–245.

Khain, A. P., D. Rosenfeld, and A. Pokrovsky (2001), Simulating convective clouds with sustained supercooled liquid water down to −37.5°C using a spectral microphysics model, *Geophys. Res. Lett.*, *28*, 3887–3890.

Lynn, B., A. Khain, D. Rosenfeld, and W. L. Woodley (2007), Effects of aerosols on precipitation from orographic clouds, *J. Geophys. Res.*, *112*, D10225, doi:10.1029/2006JD007537.

McFarquhar, G. M., and A. J. Heymsfield (2001), Parameterizations of INDOEX microphysical measurements and calculations of cloud susceptibility: Applications for climate studies, *J. Geophys. Res.*, *106*, 28,675–28,698.

Rosenfeld, D. (2000), Suppression of rain and snow by urban and industrial air pollution, *Science*, *287*(5459), 1793–1796.

Rosenfeld, D., and A. Givati (2006), Evidence of orographic precipitation suppression by air pollution induced aerosols in the western U. S., *J. Appl. Meteorol.*, *45*, 893–911.

Rosenfeld, D., and G. Gutman (1994), Retrieving microphysical properties near the tops of potential rain clouds by multispectral analysis of AVHRR data, *Atmos. Res.*, *34*, 259–283.

Rosenfeld, D., and I. M. Lensky (1998), Satellite-based insights into precipitation formation processes in continental and maritime convective clouds, *Bull. Am. Meteorol. Soc.*, *79*, 2457–2476.

Rosenfeld, D., and C. W. Ulbrich (2003), Cloud microphysical properties, processes, and rainfall estimation opportunities, in *Radar and Atmospheric Science: A Collection of Essays in Honor of David Atlas*, chap. 10, edited by R. M. Wakimoto and R. Srivastava, *Meteorol. Monogr.*, *52*, 237–258, AMS, Boston.

Rosenfeld, D., W. L. Woodley, T. W. Krauss, and V. Makitov (2006), Aircraft microphysical documentation from cloud base to anvils of hailstorm feeder clouds in Argentina, *J. Appl. Meteorol.*, *45*, 1261–1281, September.

Rosenfeld, D., J. Dai, X. Yu, Z. Yao, X. Xu, X. Yang, and C. Du (2007), Inverse relations between amounts of air pollution and orographic precipitation, *Science*, *315*, 1396–1398, March.

Woodley Weather Consultants (2005), *The Use of a Cloud Physics Aircraft for the Mapping of Pollution Aerosols Detrimental to Winter Orographic Precipitation Over the California Sierra Nevada*, Calif. Energy Com., PIER Energy-Related Environ. Res. CEC-500-2005-205, White Fir Court, Littlton, Colorado.

Woodley Weather Consultants (2007), *Physical/Statistical and Modeling Documentation of the Effects of Urban and Industrial Air Pollution in California on Precipitation and Stream Flows,* Calif. Energy Com., PIER Energy-Related Environ. Res. Prog. CEC-500-2007-019, White Fir Court, Littlton, Colorado.

Yum, S. S., and J. G. Hudson (2002), Maritime/continental microphysical contrasts in stratus, *Tellus, Ser. A and Ser. B*, *54B*, 61–73.

D. Axisa, Seeding Operation and Atmospheric Research, P.O. Box 130, Plains, TX 79355, USA.

E. Freud, A. Givati, and D. Rosenfeld, Institute of Earth Sciences, The Hebrew University of Jerusalem, Givat Ram, Jerusalem 91904, Israel. (daniel.rosenfeld@huji.ac.il)

J. G. Hudson, Atmospheric Sciences Division, Desert Research Institute, University of Nevada, 2215 Raggio Parkway Reno, NV 89512, USA. (hudson@dri.edu)

W. L. Woodley, Woodley Weather Consultants, 11 White Fir Court, Littleton, CO 80127, USA.